Synthesis and Electronic Properties of Anthraquinone-, Tetracyanoanthraquinodimethane-, and Perylenetetracarboxylic Diimide-Functionalized Poly(3,4-ethylenedioxythiophenes)

José L. Segura,*[,†,‡] Rafael Gómez,[†] Raúl Blanco,[†] Egon Reinold,[‡] and Peter Bäuerle*[,‡]

Departamento de Química Orgánica, Facultad de Química, Universidad Complutense, E-28040, Madrid, Spain, and Department of Organic Chemistry II (Organic Materials and Combinatorial Chemistry), University of Ulm, Albert-Einstein Allee 11, 89081 Ulm, Germany

Received January 26, 2006. Revised Manuscript Received March 23, 2006

Poly(3,4-ethylenedioxythiophene) (PEDOT) is frequently used as a conducting layer in various applications, e.g., organic devices. However, the modification of the precursor 3,4-ethylenedioxythiophene (EDOT) has only very recently received some attention. Here, we report the efficient synthesis of chloromethyl-functionalized EDOT **3** which is a versatile intermediate to easily access functionalized EDOT derivatives and their corresponding PEDOTs bearing, e.g., electron acceptor groups. In this respect, novel EDOT derivatives **11**−**13** covalently functionalized with 9,10-anthraquinone (AQ), perylenetetracarboxylic diimide (PTCDI), and 11,11,12,12-tetracyano-9,10-anthraquinodimethane (TCAQ) have been synthesized and potentiodynamically electropolymerized. The redox properties of the new polymers **P11**−**P13** were investigated, indicating that in the hybrid systems, both the PEDOT backbone and the acceptor moieties basically retain their individual properties. In the same line, optical spectra reveal the superimposition of the optical transitions of the individual π-systems.

Introduction

Although in 1967 2,5-diethoxycarbonyl-3,4-ethylenedioxythiophene was synthesized as the first EDOT derivative,[1] it was not until 1988 that the first synthesis of EDOT itself was carried out by scientists at Bayer company.[2] Since then, poly(3,4-ethylenedioxythiophene) (PEDOT) and its derivatives have been the subject of considerable interest motivated by the unique combination of moderate band gap and low oxidation potential, giving rise to an exceptionally stable oxidized conducting state. High conductivity[3] and optical transparency in the visible spectral range[4] have allowed the development of many applications of PEDOT including antistatic coatings, electrode materials in super capacitors, and hole injection layers in organic light-emitting diodes (OLED) or organic solar cells (OSC).[5,6] The significance and main applications of PEDOT and its derivatives have been discussed at length in recent reviews.[7−9]

Consequently, the chemistry of the EDOT monomer itself and the modification of the basic structure have been developed in parallel. Very recently, Roncali and co-workers have reviewed the opportunities offered by the EDOT building block for the design and synthesis of new classes of functional π-conjugated systems.[10] In this respect, due to the specific electronic properties of EDOT, which combine electropolymerization at low potentials and high reactivity of the resulting radical cations, further work has been devoted to the synthesis of hybrid systems containing typical units of conducting polymers such as thiophenes or phenylenes and EDOT. Nevertheless, only few examples are known in which electron acceptor moieties have been covalently linked as pendant groups to the conjugated PEDOT backbone.[11]

A modification of the basic EDOT structure is only possible by substituents at the ethylenedioxy bridge. To achieve solubility of the resulting polymer, differently substituted EDOTs bearing alkyl,[12] oligooxyethylene,[13] alkylsulfonate,[14] or perfluoroalkyl groups[15] have been reported. Despite the fact that functionalized polypyrroles[16] and

* To whom correspondence should be addressed. Phone (J.L.S.): +34-91-3945142. E-mail: segura@quim.ucm.es. Phone (P.B.): +49-731-50-22850. E-mail: peter.baeuerle@uni-ulm.de.

[†] Universidad Complutense.

[‡] University of Ulm.

(1) Gogte, V. N.; Shah, L. G.; Tilak, B. D.; Gadekar, K. N.; Sahasrabudhe, M. B. *Tetrahedron* **1963**, *23*, 2437.
(2) Jonas, F.; Heywang, G.; Schmidtberg, W.; Heinze, J.; Dietrich, M. Bayer AG, Eur. Patent 339 340, 1988.
(3) Aleshin, A. N.; Kiebooms, R.; Heeger, A. J. *Synth. Met.* **1999**, *101*, 369.
(4) (a) Jonas, F.; Shrader, L. *Synth. Met.* **1991**, *41*−*43*, 83. (b) Heywang, G.; Jonas, F. *Adv. Mater.* **1992**, *4*, 116.
(5) Kang, T. S.; Harrison, B. S.; Bouguettaya, M.; Foley, T. J.; Boncella, J. M.; Schanze, K. S.; Reynolds, J. R. *Adv. Funct. Mater.* **2003**, *13*, 205.
(6) Brabec, C. J.; Sariciftci, N. S.; Hummelen, J. C. *Adv. Funct. Mater.* **2001**, *11*, 15.
(7) Groenendaal, L.; Jonas, F.; Freitag, D.; Pielartzik, H.; Reynolds, J. R. *Adv. Mater.* **2000**, *12*, 481.
(8) Groenendaal, L.; Zotti, G.; Aubert, P.-H.; Waybright, S. M.; Reynolds, J. R. *Adv. Mater.* **2003**, *15*, 855.
(9) Kirchmeyer, S.; Reuter, K. *J. Mater. Chem.* **2005**, *15*, 2077.
(10) Roncali, J.; Blanchard, P.; Frère, P. *J. Mater. Chem.* **2005**, *15*, 1589.
(11) (a) Ko, H.-C.; Kang, M.; Moon, B.; Lee, H. *Adv. Mater.* **2004**, *16*, 1712. (b) Czardybon, A.; Zak, J.; Laplowski, M. *Pol. J. Chem.* **2004**, *78*, 1533.
(12) (a) Schottland, P.; Stephan, O.; Le Gall, P. Y.; Chevrot, C. *J. Chem. Phys. Phys.-Chim. Biol.* **1998**, *95*, 1258. (b) Czardybon, M.; Lapkowsky, M. *Synth. Met.* **2001**, *119*, 161. (c) Sapp, S. A.; Sotzing, G. A.; Reynolds, J. R. *Chem. Mater.* **1998**, *10*, 2101.
(13) Perepichka, I.; Levillain, E.; Sallé, M.; Roncali, J. *Chem. Mater.* **2002**, *14*, 449.

10.1021/cm0602085 CCC: $33.50
Published on Web 05/20/2006

polythiophenes[17] have been widely explored and convincingly demonstrate that by covalent attachment of functional groups at the conjugated backbone novel properties and applications can be created, only very few examples of functionalized PEDOTs have been reported so far. As intermediates, hydroxymethyl-substituted EDOT **I** and iodoalkyl derivatives **II** and **III**, which were subsequently prepared from **I**,[18] were used (Chart 1), whereby the synthesis of EDOT **I** is quite problematic. An isomeric hydroxy-substituted 3,4-propylenedioxythiophene (ProDOT) is formed as a byproduct which can be separated only after tedious chromatographic purification. Starting from EDOT **I**, by a Williamson ether synthesis, cyanobiphenyl-functionalized EDOT **IV** was prepared in order to produce better contrast in electrochromic devices.[19] Three examples of EDOTs functionalized with redox active groups are known. Reaction of EDOT **I** with ferrocene propionic acid gave EDOT **V**.[20] However, ferrocene-EDOT **V** could not successfully be electropolymerized to the corresponding electron donor-functionalized PEDOT probably due to the interfering redox chemistry of the easily oxidizable ferrocene moieties. To obtain polymer films, copolymerization with other EDOT monomers was necessary. A PEDOT derivatized with the strong electron donor group tetrathiafulvalene (TTF) was obtained[21] by a postfunctionalization method.[22] Intermediate EDOTs **II** and **III** could be successfully electropolymerized under the retention of the reactive iodo group and were then reacted in a polymer-analogous reaction with a TTF-precursor molecule to form TTF-PEDOT **VI**, which was used in amperometric sensors to recognize heavy metals in solution. The only known PEDOTs having pendant electron-accepting groups were prepared from viologen-functionalized EDOTs **VII**, providing interesting electrochromic properties.[11]

In the course of our work to further develop the synthesis and chemistry of EDOT derivatives,[23] in this article we report the efficient synthesis of reactive chloromethyl-substituted EDOT **3** as a novel and convenient intermediate for functionalized (P)EDOTs. By nucleophilic substitution reactions electron acceptor groups such as 9,10-anthraquinone (AQ), perylenetetracarboxylic diimide (PTCDI), and 11,11,12,12-tetracyano-9,10-anthraquinodimethane (TCAQ) were covalently linked to the EDOT core. The new EDOT derivatives **11**−**13** showed good tendency to electropolymerize to the corresponding acceptor-functionalized PEDOTs **P11**−**P13**, representing interesting electron donor−acceptor hybrid materials. In the search for donor−acceptor systems to investigate photoinduced energy and electron transport processes, pendant electron acceptor groups such as fullerenes,[24,25] anthraquinone,[26] tetracyanoanthraquinodimethane,[27] or perylenetetracarboxylic diimide derivatives[28,29] have so

Chart 1

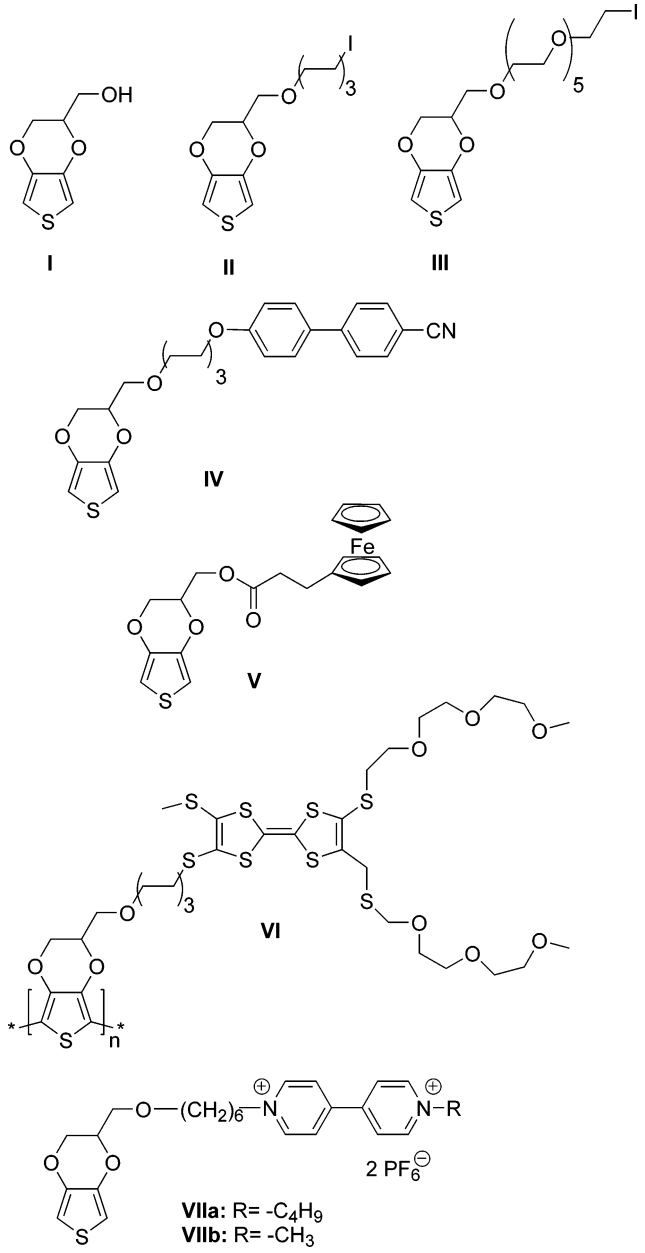

(14) (a) Stephan, O.; Schottland, P. Y.; Le Gall, P. Y.; Chevrot, C. *J. Chem. Phys. Phys.-Chim. Biol.* **1998**, *95*, 1168. (b) Trau-Van, F.; Carrier, M.; Chevrot, C. *Synth. Met.* **2004**, *142*, 251. (c) Cutler, C. A.; Bouguettaya, M.; Kang, T.-S.; Reynolds, J. R. *Chem. Mater.* **2005**, *38*, 3068.

(15) (a) Ha, Y.-H.; Nikolov, N.; Dulcey, C.; Wang, S.-C.; Mastrangelo, J.-; Shashidhar, R. *Synth. Met.* **2004**, *144*, 101. (b) Zuo, L.; Qing, F.-L.; Meng, W.-D.; Huang, X.; Zhang, S.; Wu, Q. *J. Fluorine Chem.* **2004**, *125*, 1441.

(16) Garnier, F.; Korri, H.; Hmyene, M.; Yassar, A. *Polym. Prepr.* **1994**, *35*, 206.

(17) For reviews on polythiophene derivatives, see: (a) Roncali, J. *Chem. Rev.* **1992**, *92*, 711. (b) McCullough, R. D. *Adv. Mater.* **1998**, *10*, 93. (c) Perepichka, I. F.; Perepichka, D. F.; Meng, H.; Wudl, F. *Adv. Mater.* **2005**, *17*, 2281.

(18) Besbes, M.; Trippé, G.; Levillain, E.; Mazari, M.; Le Derf, F.; Perepichla, I.; Gorgues, A.; Sallé, M.; Roncali, J. *Adv. Mater.* **2001**, *13*, 1249.

(19) Krishnamoorthy, K.; Kanungo, M.; Contractor, A. Q.; Kumar, A. *Synth. Met.* **2001**, *124*, 471.

(20) Brisset, H.; Navarro, A.-E.; Moustrou, C.; Perepichka, I. F.; Roncali, J. *Electrochem. Commun.* **2004**, *6*, 249.

(21) Lyskawa, J.; Le Derf, F.; Levillain, E.; Mzari, M.; Sallé, M.; Dubois, L.; Viel, P.; Bureau, C.; Palacin, S. *J. Am. Chem. Soc.* **2004**, *126*, 12194.

(22) (a) Bäuerle, P.; Hiller, M.; Dcheib, S.; Sokolowski, M.; Umbach, E. *Adv. Mater.* **1996**, *8*, 214. (b) Wenzel, H.-P.; Kossmehl, G.; Schneider, J.; Plieth, W. *Macromolecules* **1995**, *28*, 5575.

(23) (a) Caras-Quintero, D.; Bäuerle, P. *Chem. Commun.* **2002**, 2690. (b) Caras-Quintero, D.; Bäuerle, P. *Chem. Commun.* **2004**, 926.

(24) For reviews on conjugated polymers with pendant fullerene groups, see: (a) Cravino, A.; Sariciftci, N. S. *J. Mater. Chem.* **2002**, *12*, 1931. (b) Roncali, J. *Chem. Soc. Rev.* **2005**, *34*, 483.

(25) Yamazaki, T.; Murata, Y.; Komatsu, K.; Furukawa, K.; Morita, M.; Maruyama, N.; Yamao, T.; Fujita, S. *Org. Lett.* **2004**, *6*, 4865.

Scheme 1

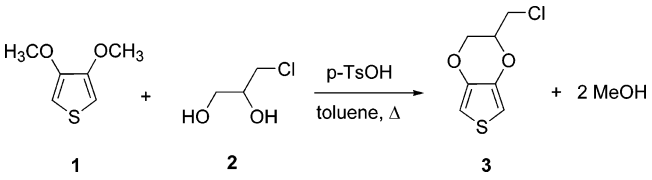

far been covalently linked to conjugated polymer backbones such as poly(phenylenevinylene) (PPV), poly(phenyleneethynylene) (PPE), or polythiophene derivatives, but not yet to PEDOT.

Results and Discussion

Synthesis of the Functionalized EDOTs 11−13. For the modification of the EDOT system it is especially interesting to synthesize easily accessible EDOT derivatives bearing reactive groups which might be used to further covalently link pendant groups to the EDOT system. In this respect, the straightforward synthesis of chloromethyl-EDOT **3** was developed by reacting 3,4-dimethoxythiophene (**1**)[30] and commercially available 3-chloro-1,2-propanediol (**2**) in an acid-catalyzed transetherification reaction[23b] (62% yield, Scheme 1). By Mitsunobu reaction of 3,4-dihydroxy-2,5-carbethoxythiophene and the same diol **2** a dicarbethoxy derivative of **3** was already synthesized in 65% yield[23a] which then had to be hydrolyzed and decarboxylated to finally give EDOT **3**. Nevertheless, both procedures to synthesize chloromethyl-EDOT **3** should be advantageous and more convenient over the preparation of the so far used hydroxymethyl−EDOT **I**.

Activated EDOT derivative **3** can now be easily reacted with many functional groups in typical nucleophilic substitution reactions. Thus, we first have carried out the synthesis of electron acceptor systems such as 9,10-anthraquinone (AQ) **5**, 11,11,12,12-tetracyano-9,10-anthraquinodimethane (TCAQ) **7**, or perylenetetracarboxylic diimide (PTCDI) **10** derivatives bearing phenolic groups which should react in a Williamson etherification with chloromethyl-EDOT **3** (Scheme 2).

Anthraquinone **5** was prepared in 48% yield by Williamson etherification of anthraflavic acid (**4**) and one equivalent of hexylbromide under basic conditions and had to be separated from disubstitution product **6** by column chromatography. TCAQ derivative **7** was obtained in 89% yield from anthraquinone **5** by reaction with malononitrile in the presence of Lehnert's reagent ($TiCl_4$ and pyridine in chloroform).[31] The unsymmetrical PTCDI derivative *N*-(10-nonadecyl)-3,4,9,10-perylenetetracarboxylic acid 3,4-anhydride-9,10-imide (**8**) can be obtained according to the literature,[32] by partial hydrolysis of the corresponding symmetrical perylenetetracarboxylic diimide which in turn is readily accessible from the commercially available perylenetetracarboxylic dianhydride. Reaction of **8** with *p*-aminophenol (**9**) in imidazole at 180 °C in the presence of zinc acetate gave the asymmetrically substituted PTCDI derivative **10** bearing a reactive phenolic group.

Consequently, the coupling of AQ **5** to chloromethyl-EDOT **3** was carried out under basic conditions and a catalytic amount of potassium iodide in DMF at 100 °C to form 9,10-anthraquinone-functionalized EDOT **11** in 77% yield (Scheme 3). The reaction of PTCDI derivative **10** with EDOT **3** under the same conditions led to PTCDI-functionalized EDOT **12**[33] in a moderate yield of 34%. Due to the lower stability of TCAQ derivative **7** in basic media, its reaction with EDOT **3** under Williamson etherification conditions failed. Therefore, similarly to the preparation of TCAQ derivative **7**, we reacted AQ-EDOT **11** with malononitrile in the presence of Lehnert's reagent to obtain TCAQ-EDOT **13** in 62% yield.

Alkyl side chains in the acceptor units of EDOTs **11**−**13** provide solubility and allow their full characterization by NMR, optical, and electrochemical methods. ^{1}H NMR spectra of the three EDOT monomers show common features arising from the EDOT unit. Due to the asymmetry of the substituted 2,3-dihydrothieno[3,4-b][1,4]dioxin fragments, thiophene protons appear as an AB system centered at 6.38−6.30 ppm with coupling constants of 3.92−3.72 Hz. The protons at position 2 of the dioxin ring appear as a complex multiplet at 4.4−4.1 ppm, whereas H-3 is deshielded to 4.6−4.5 ppm. Besides these common features, each derivative exhibits characteristic signals arising from the acceptor unit. For example, in the ^{1}H NMR spectrum of PTCDI-EDOT **12** the expected doublet and multiplet at low fields (8.7−8.6 ppm) for the aromatic perylene protons are visible. On the other hand, the phenyl spacer gives rise to two doublets with a characteristic ortho coupling of 8.8 Hz. The spectrum is completed by signals at higher fields for the nonyl chains and the multiplet at 5.23 ppm for the proton directly linked to the imide nitrogen. Due to the structural similarity of the acceptor fragments in AQ-EDOT **11** and in TCAQ-EDOT **13**, their ^{1}H NMR spectra are comparable. Because of the vicinity to the deshielding carbonyl or dicyanovinylene groups, respectively, two close doublets with a characteristic ortho coupling of 8.6 Hz for **11** and 8.8 Hz for **13** appear at low field (8.16, 8.13 ppm for **11**; 8.12, 8.10 ppm for **13**) and correspond to anthraquinone protons 4 and 8. Doublets for similarly deshielded protons 1 and 5 appear at slightly

(26) (a) Iraqi, A.; Crayston, J. A.; Walton, J. C. *J. Mater. Chem.* **1998**, *8*, 31. (b) Luzzati, S.; Scharber, M.; Catellani, M.; Lupsac, N.-O.; Giacalone, F.; Segura, J. L.; Martín, N.; Neugebauer, H.; Sariciftci, N. S. *Synth. Met.* **2003**, *139*, 731.
(27) (a) Zerza, G.; Cravino, A.; Neugebauer, H.; Sariciftci, N. S.; Gómez, R.; Segura, J. L.; Martín, N.; Svensson, M.; Andersson, M. R. *J. Phys. Chem. A* **2001**, *105*, 4172. (b) Catellani, M.; Luzzati, S.; Lupsac, N.-O.; Mendichi, R.; Consonni, R.; Giacalone, F.; Segura, J. L.; Martín, N. *Thin Solid Films* **2004**, *451*, 2. (c) Giacalone, F.; Segura, J. L.; Martín, N.; Catellani, M.; Luzzati, S.; Lupsac, N.-O. *Org. Lett.* **2003**, *5*, 1669. (d) Catellani, M.; Luzzati, S.; Lupsac, N.-O.; Mendichi, R.; Consonni, R.; Famulari, A.; Meille, S. V.; Giacalone, F.; Segura, J. L.; Martín, N. *J. Mater. Chem.* **2004**, *14*, 67.
(28) Neuteboom, E. E.; van Hal, P. A.; Janssen, R. A. J. *Chem. Eur. J.* **2004**, *10*, 3907.
(29) (a) You, C. C.; Saha-Möller, C. R.; Würthner, F. *Chem. Commun.* **2004**, 2030. (b) Chen, S.; Liu, Y.; Qiu, W.; Sun, X.; Ma, Y.; Zhu, D. *Chem. Mater.* **2005**, *17*, 2208.
(30) Langeveld-Voss, B. M. W.; Janssen, R. A. J.; Meijer, E. W. *J. Mol. Struct.* **2000**, *521*, 285.
(31) (a) Lehnert, W. *Tetrahedron Lett.* **1970**, 4723. (b) Lehnert, W. *Synthesis* **1974**, 667.
(32) (a) Langhals, H. *Heterocycles* **1995**, *40*, 477. (b) Kaiser, H.; Lindler, J.; Langhals, H. *Chem. Ber.* **1991**, *124*, 529.
(33) Segura, J. L.; Gómez, R.; Reinold, E.; Bäuerle, P. *Org. Lett.* **2005**, *7*, 2345.

Scheme 2

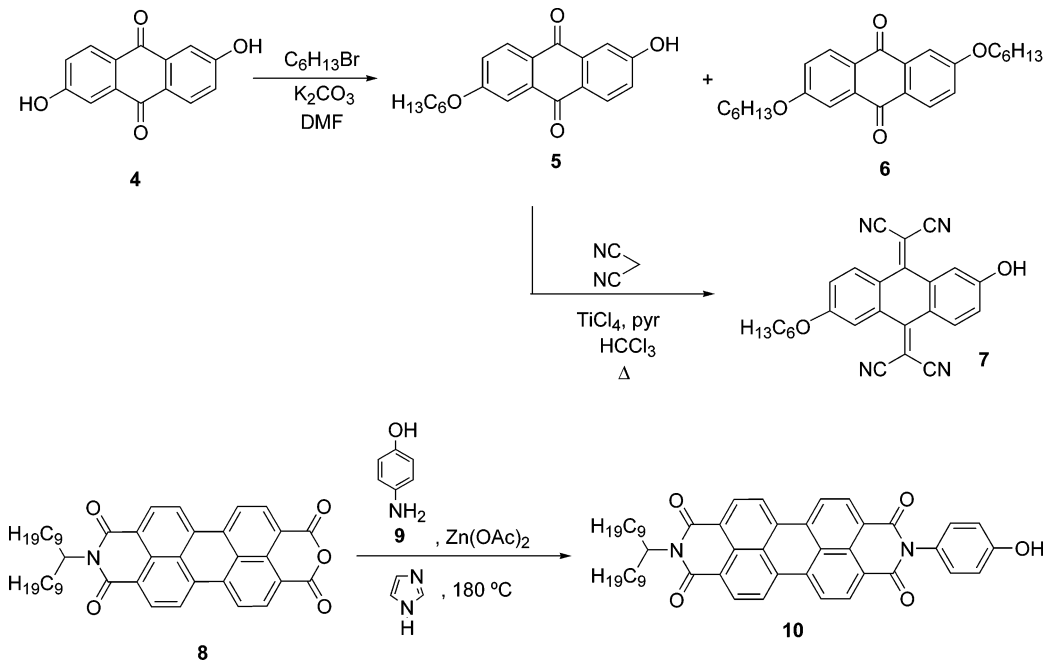

Scheme 3

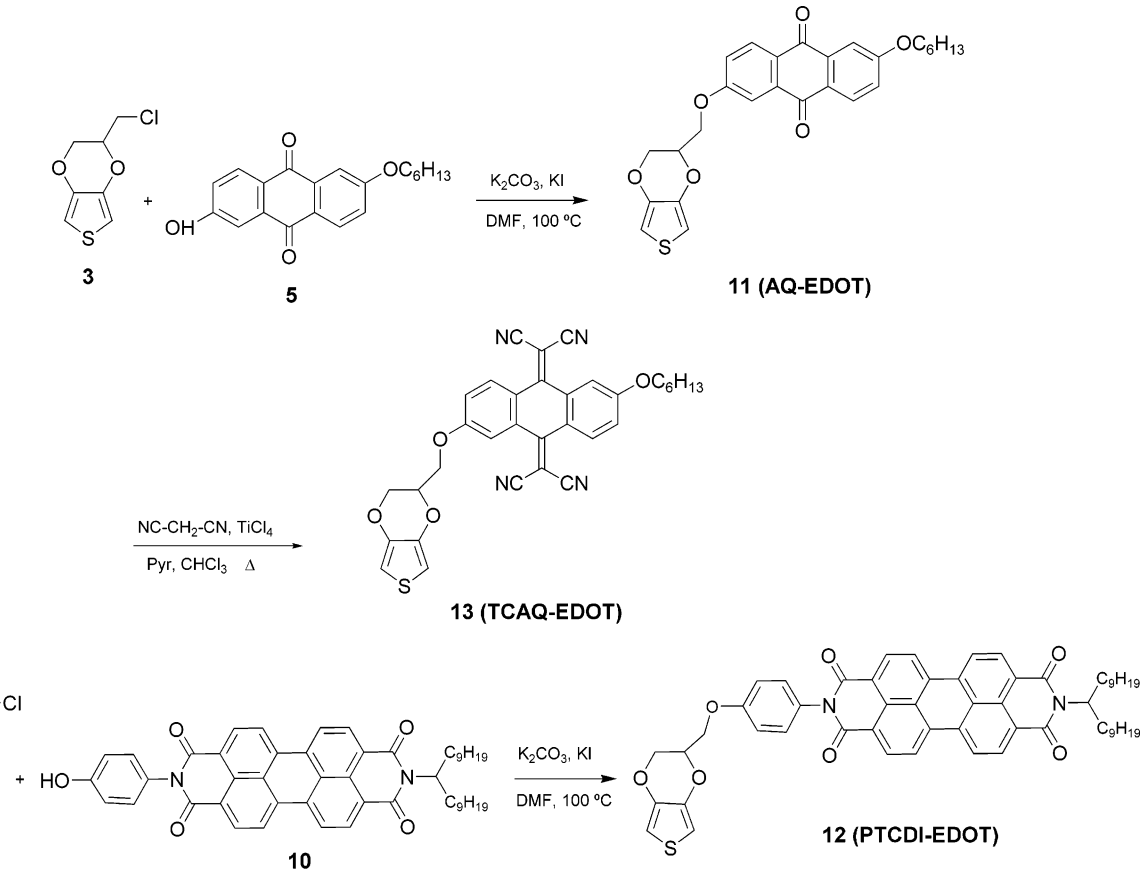

higher field (7.64, 7.61 ppm for **11**; 7.75, 7.70 ppm for **13**) comprising a meta coupling of 2.6 Hz for **11** and 2.4 Hz for **13**, respectively. The remaining protons 4 and 7 show multiplets at 7.24−7.14 ppm for both compounds.

Despite the remarkable resemblance in their ^{1}H NMR spectra, the ^{13}C NMR spectra of EDOTs **11** and **13** show peculiarities coming from the carbonyl and dicyanovinylene groups, respectively. A signal at 181.9 ppm is observed for C9 and C10 of the carbonyl group in **11** while the presence of dicyanovinylene groups in **13** is confirmed by signals at 114−113 ppm (vinylic C) and 82−80 ppm (CN). C9 and C10 in TCAQ-EDOT **13** appear at higher field (160−159 ppm) compared to AQ-EDOT **11**.

FTIR spectra of the three acceptor-functionalized EDOTs **11**−**13** further prove their structures and contain the typical strong bands at 1684 cm^{-1} for carbonyl groups in AQ-EDOT

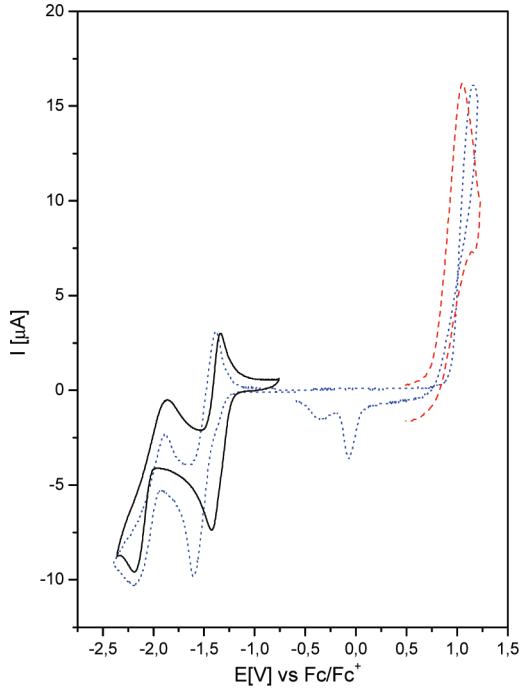

Figure 1. Cyclic voltammogram of anthraquinone-functionalized AQ-EDOT **11** (blue dotted line) and of parent compounds Me-EDOT **16** (red dashed line) and AQ **6** (black solid line) in dichloromethane/TBAHPF (0.1 M) at 20 °C, scan rate of 100 mV/s, Pt disk working electrode, potentials vs Fc/Fc^+.

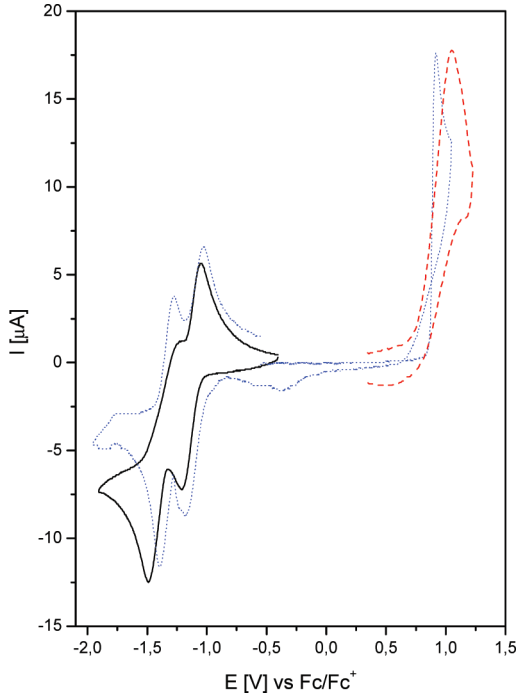

Figure 2. Cyclic voltammogram of perylenetetracarboxylic diimide-functionalized PTCDI-EDOT **12** (blue dotted line) and of parent compounds Me-EDOT **16** (red dashed line) and PTCDI **14** (black solid line) in dichloromethane/TBAHPF (0.1 M) at 20 °C, scan rate of 100 mV/s, Pt disk working electrode, potentials vs Fc/Fc^+.

11, at 1699 and 1653 cm^{-1} for imide groups in PTCDI-EDOT **12**, and 2222 cm^{-1} for cyano groups in TCAQ-EDOT **13**.

Redox Properties of the Acceptor-Functionalized EDOT Derivatives. The electrochemical behavior of the new EDOT derivatives **11**−**13** was investigated by cyclic voltammetry (CV) in dichloromethane (DCM) and tetrabutylammonium hexafluorophosphate (TBAHFP) as electrolyte (Figures 1−3). Reduction and oxidation potentials were measured relative to the internal standard ferrocene−ferricenium (Fc/Fc^+) (Table 1). In the positive potential regime, CVs of **11**, **12**, and **13** show a typical irreversible anodic peak at 1.16, 0.92, and 1.16 V, respectively, corresponding to the formation of EDOT radical cations. These values are comparable to methyl-substituted EDOT (Me-EDOT), which exhibits an irreversible anodic peak at 1.03 V under identical conditions.[34] The higher oxidation potential for AQ-EDOT **11** and TCAQ-EDOT **13** with respect to that of Me-EDOT is due to the close vicinity of the acceptor to the EDOT system, thus decreasing electron density. A different behavior was observed for PTCDI-EDOT **12** which exhibits a lower oxidation potential in comparison with the other monomers. Many PTCDI derivatives substituted at the imide nitrogen have already been investigated and it has been observed that the imide substituent has a negligible influence on the electronic properties of perylenebisimides because of the presence of nodes of the HOMO and LUMO at the imide nitrogen.[35] Thus, perylenebisimides can be regarded as closed chromophoric systems whose electronic properties remain

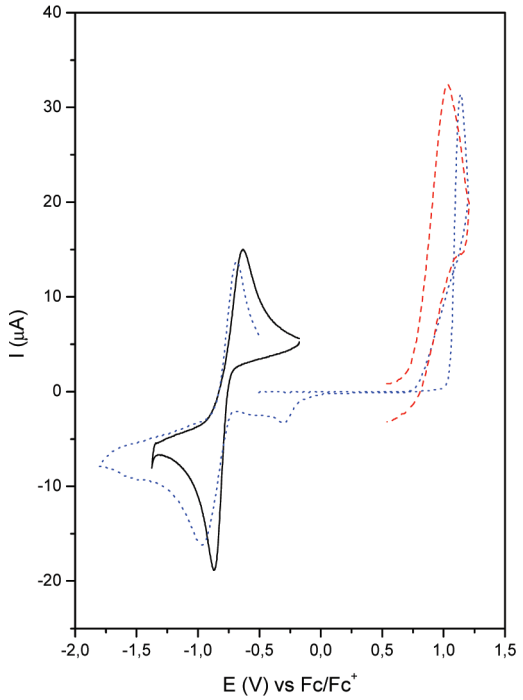

Figure 3. Cyclic voltammogram of tetracyanoanthraquinodimethane-functionalized TCAQ-EDOT **13** (blue dotted line) and of parent compounds Me-EDOT **16** (red dashed line) and TCAQ **15** (black solid line) in dichloromethane/TBAHPF (0.1 M) at 20 °C, scan rate of 100 mV/s, Pt disk working electrode, potentials vs Fc/Fc^+.

unaltered by the imide substituent.[36] In this regard, in compound **12** no electronic influence of the PTCDI moiety in the EDOT system is expected as it is also observed in the UV−Vis spectra. Thus, considering the electron-withdrawing

(34) Caras-Quintero, D. Ph.D. Thesis, University of Ulm, 2003.
(35) Würthner, F. *Chem. Commun.* **2004**, 1564.
(36) Langhals, H.; Demmig, S.; Huber, H. *Spectrochim. Acta* **1998**, *44A*, 1189.

Table 1. Electrochemical Properties of the Acceptor-Functionalized EDOTs 11−13 and Reference Compounds Me-EDOT 16, AQ 6, PTCDI 14, and TCAQ 15

compound[a]	E°_{red2} (V)	E°_{red1} (V)	E^{p}_{ox} (V)
AQ-EDOT **11**	−1.89	−1.37	1.16
PTCDI-EDOT **12**	−1.33	−1.11	0.92
TCAQ-EDOT **13**		$E^{p}_{red} = -0.97$[b]	1.16
		$E^{p}_{ox} = -0.68$[b]	
Me-EDOT **16**			1.03
AQ **6**	−1.88	−1.22	
PTCDI **14**	−1.37	−1.15	
TCAQ **15**		$E^{p}_{red} = -0.87$[b]	
		$E^{p}_{ox} = -0.64$[b]	

[a] $c = 5 \times 10^{-3}$ mol L^{-1} in dichloromethane-TBAHFP (0.1 M) vs Fc/Fc^{+} at 100 mV s^{-1}. [b] Despite the chemical reversibility of the reduction of the acceptor group, a bigger difference between the cathodic and anodic peak potential has been found (ΔE > 200 mV) than expected for an electrochemically reversible redox couple ($\Delta E \leq 60$ mV). This is due to a conformational change upon reduction.

inductive through bond effect of the phenoxy spacer, a higher potential should be expected. The opposite effect observed experimentally could be explained in terms of (i) $\pi-\pi$ interaction of the EDOT unit and the PTCDI or (ii) by an electrocatalytic effect of the planar acceptor similar to that recently reported by Zotti et al. for different thiophene-based monomers in the presence of terthiophene promoters.[37]

In all three cases, a potential scan toward negative potentials reveals reversible reduction waves due to the acceptor moieties, indicating the formation of stable radical anions and dianions, respectively. According to the acceptor strength of the functional group, the weakest acceptor AQ in AQ-EDOT **11** is reduced at the lowest potential ($E^{\circ}_{red1} = -1.37$ V, $E^{\circ}_{red2} = -1.89$ V), PTCDI-EDOT **12** at $E^{\circ}_{red1} = -1.11$ V and $E^{\circ}_{red2} = -1.33$ V whereas TCAQ-EDOT **13** shows the least negative potential ($E^{p}_{red} = -0.97$, $E^{p}_{ox} = -0.68$).[38] The reduction potentials observed for the hybrid systems **11**−**13** are only slightly shifted in comparison to those of the parent compounds AQ **6** ($E^{\circ}_{red1} = -1.22$ V and $E^{\circ}_{red2} = -1.88$ V),[39] PTCDI **14** ($E^{\circ}_{red1} = -1.15$ V, $E^{\circ}_{red2} = -1.37$ V),[40,41] and TCAQ **15** ($E^{p}_{red} = -0.87$, $E^{p}_{ox} = -0.64$),[42] suggesting that the acceptor moieties retain their individual electrochemical behavior (Chart 2).

It is worth mentioning that for the three monomers a clear trace crossing is observable upon oxidation, which points to a fast formation of oligomeric or polymeric material on the electrode even after the first oxidation scan. Thus, the back sweep of the CV after oxidation shows reduction peaks between 0 and −0.5 V corresponding to the reduction of the initially deposited oligomeric materials and evidence for the nucleation process on the surface of the electrode.

Electrochemical Polymerization of Acceptor-Functionalized EDOTs 11−13 to the Corresponding PEDOTs P11−P13 and Characterization of the Electronic Properties. *Electrochemical Polymerization of the Monomers.* Conjugated polyheterocycles typically are prepared via chemical or electrochemical oxidation.[43] However, electropolymerization provides the advantage for the direct growth of polymeric thin films on metal or transparent electrodes ready for electrochemical and spectroelectrochemical characterizations.[44,45] Thus, we carried out potentiodynamic electropolymerization of acceptor-functionalized monomers **11**−**13** in 5×10^{-3} M solutions in dichloromethane and 0.1 M TBAHPF as electrolyte by repeated scanning (Figure 4a−6a). Typically, positive turnover potentials of 1.1 V just above the peak potential of the irreversible oxidation wave of the monomers were applied, whereas the negative turnover (<−1.0 V) was chosen in a way that not yet reduction of the acceptor moieties occurred. The growth of the corresponding conducting polymer films, AQ-PEDOT **P11**, PTCDI-PEDOT **P12**, and TCAQ-PEDOT **P13** (Figures 4a−6a, Scheme 4) is reflected by the appearance of a novel redox wave at lower potentials than the monomer oxidation which gradually increases in subsequent potential cycles. The thickness of the electroactive polymer film is steadily increased and can be controlled by the number of cycles. The polymers obtained were strongly adhered to the working electrode and provided apparently homogeneous films.

Electrochemical Characterization of the Polymer Films. The acceptor-functionalized PEDOTs **P11**−**P13** were electrochemically characterized in an electrolyte free of monomer (acetonitrile/TBAHFP 0.1 M) (Figures 4b−6b). In the CVs of **P11**, a broad redox wave corresponding to the p-doping/dedoping of the PEDOT backbone is clearly separated from those of the acceptor units. The charging of the conjugated backbone, which is concomitant with the transition from the semiconducting to the conducting state, starts at around $E_{lim} = -0.76$ V (**P11**) and maximum current is found at $E^{p}_{ox1} = -0.20$ V (**P11**) (Table 2). These values are distinctly more positive than those of the nonfunctionalized parent polymer P(Me-EDOT) (**P16**, $E_{lim} = -0.94$ V, $E^{p}_{ox1} = -0.73$ V),[34] indicating the electron-withdrawing effect of the pendant anthraquinone groups.

At this point, it is worth mentioning that the transition between the polaronic and bipolaronic state is a continuous transition difficult to estimate from cyclic voltammetry. Therefore, in this section we will designate as $PEDOT^{Ox}$ the oxidized form of PEDOT. On the other hand, in the section dedicated to the optical properties of the polymer films we will mention explicitly polarons and bipolarons considering that spectroelectrochemistry allows us to unambiguously assign the absorption corresponding to these species.

For PTCDI-PEDOT (**12**) a large oxidation peak is observed for the PEDOT moiety which is suggestive of a uniform material (Figure 5b). This may be due to the larger

(37) Zotti, G.; Zecchin, S.; Schiavon, G.; Vercelli, B.; Berlin, A. *J. Electroanal. Chem.* **2005**, *575*, 169.
(38) Despite the chemical reversibility of the reduction of the TCAQ system, a difference between the cathodic and anodic peak potential of almost 300 mV is observed due to the conformational changes produced upon reduction. For an in-depth study of the electrochemical behavior of TCAQ, see ref 42a.
(39) (a) Hoang, P. M.; Holdcroft, S.; Funt, B. L. *J. Electrochem. Soc.* **1985**, *132*, 2129. (b) Degrand, C.; Miller, L. L. *J. Electroanal. Chem.* **1981**, *117*, 267.
(40) You, C. C.; Würthner, F. *J. Am. Chem. Soc.* **2003**, *125*, 9716.
(41) Lee, S. K.; Zu, Y.; Hermann, A.; Geerts, Y.; Müllen, K.; Bard, A. J. *J. Am. Chem. Soc.* **1999**, *121*, 3513.
(42) (a) Kini, A. M.; Cowan, D. O.; Gerson, F.; Möckel, R. *J. Am. Chem. Soc.* **1985**, *107*, 556. (b) Aumüller, A.; Hünig, S. *Liebigs Ann. Chem.* **1984**, 618.
(43) *Handbook of conducting polymers*; Skotheim, T. A., Elsenbaumer, R. L., Reynolds, J. R., Eds.; Marcel Dekker: New York, 1998.
(44) Simonet, J.; RaulBerthelot, J. *Prog. Solid State Chem.* **1991**, *21*, 1.
(45) Roncali, J. *J. Mater. Chem.* **1999**, *9*, 1875.

Chart 2. Materials Used as Reference in Cyclic Voltammetry Measurements

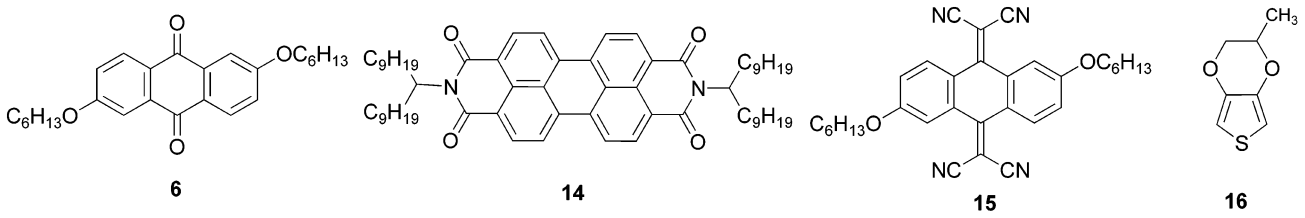

Scheme 4

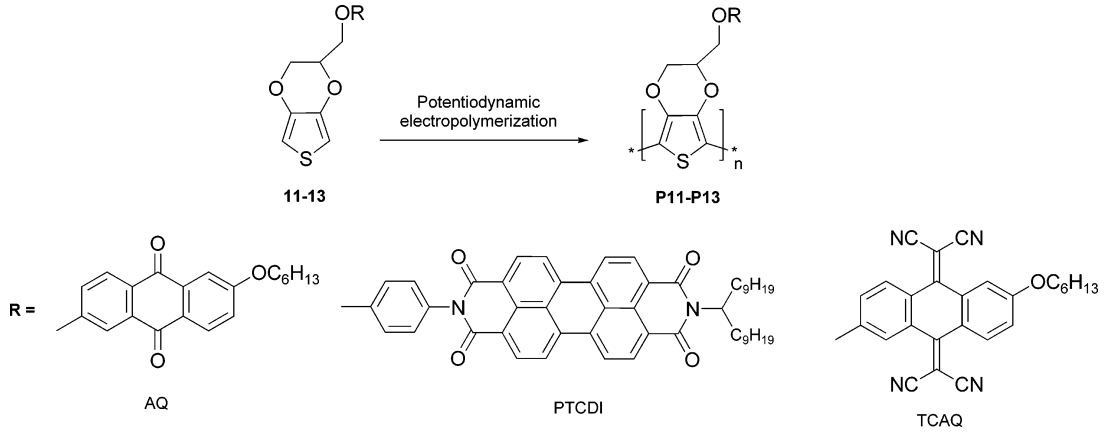

planar nature of the PTCDI moiety which is conducive to forming intraunit stacks as well as favorable surfaces for planarizing the PEDOT backbone. It is also worth mentioning that after oxidation substantial reduction current occurs at higher potentials than the initial oxidation. One possible explanation for this behavior is that oxidation of the polymer backbone may give unfavorable interactions with the PTCDI groups, thus resulting in a disruption of the polymer conformation and a destabilization of the charged state.

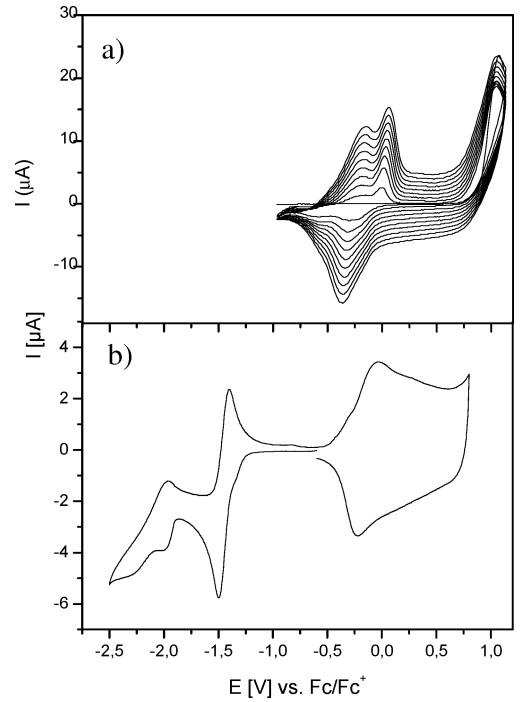

Figure 4. (a) Multisweep voltammogram (10 scans) for the polymerization of AQ-EDOT **11** in dichloromethane/TBAHPF (0.1 M) at a scan rate of 100 mV s^{-1}. (b) Electrochemical characterization of corresponding polymer **P11** in acetonitrile/TBAHPF (0.1 M) at a scan rate of 100 mV s^{-1}. All measurements were carried out at room temperature and potentials are given vs Fc/Fc^+.

Table 2. Electrochemical Properties of the Acceptor-Functionalized PEDOTs P11−P13 and Reference Compounds P(Me-EDOT) P16 and P(TCAQ-2T) P17

	acceptor		PEDOT		
compound[a]	$E°_{red2}$ (V)	$E°_{red1}$ (V)	E_{lim} (V)	E^p_{ox} (V)	E^p_{red} (V)
P(AQ-EDOT) **P11**	−1.74	−1.27	ca. −0.48	−0.03	−0.22
P(PTCDI-EDOT) **P12**	−1.19	−0.99	ca. −0.38	−0.05	−0.12
P(TCAQ-EDOT) **P13**		$E^p_{red} = -0.80$[b]	n.d.[c]	−0.14	−0.16
		$E^p_{ox} = -0.67$[b]			
P(Me-EDOT) **P16**			ca. −0.94	−0.69	−0.86
P(TCAQ-2T) **P17**		$E^p_{red} = -0.75$[b]	ca. 0.0	0.52	0.47
		$E^p_{ox} = -0.69$[b]			

[a] In acetonitrile/TBAHFP (0.1 M) vs Fc/Fc^+ at 100 mV s^{-1}. [b] Despite the chemical reversibility of the reduction of the acceptor group, a bigger difference between the cathodic and anodic peak potential has been found (ΔE > 200 mV) than expected for an electrochemically reversible redox couple ($\Delta E \leq$ 60 mV). This is due to a conformational change upon reduction. [c] Not determined due to the overlap with the TCAQ group.

At more negative potentials in the CV of polymer **P11** two (chemically) reversible redox waves are found at $E°_{red1} = -1.27$ V and $E°_{red2} = -1.74$ V. The formation of stable AQ radical anions in the polymer film occurs at slightly more positive potentials as for AQ-EDOT monomer **11** ($E°_{red1} = -1.37$ V and $E°_{red2} = -1.89$) in solution which shows that in the polymeric film charge transfer to the acceptor groups occurs. At this point it should be noted that electron transfer to pendant acceptor groups is quite frequently inhibited for acceptor-functionalized polythiophenes.[46] Exceptions are represented by viologen-[47] and AQ-functionalized poly(3-alkylthiophenes),[26a] where thickness-dependent electroactivity of the acceptor groups is noticed. In this regard, polymer

(46) (a) Ofer, D.; Crooks, R. M.; Wrighton, M. S. *J. Am. Chem. Soc.* **1990**, *112*, 7869. (b) Bäuerle, P.; Gaudl, K.-U. Götz, G. *Springer Ser. Solid State Sci.* **1992**, *107*, 384. (c) Ballarin, B.; Seeber, R.; Tassi, L.; Tonell, D. *Synth. Met.* **2000**, *114*, 279. (d) Ballarin, B.; Masiero, S.; Seeber, R.; Tonelli, D. *Synth. Met.* **2000**, *114*, 279.

(47) (a) Bäuerle, P.; Gaudl, K.-U. *Adv. Mater.* **1990**, *2*, 185. (b) Sariciftci, N. S.; Mehring, M.; Gaudl, K.-U.; Bäuerle, P.; Neugebauer, H.; Neckel, A. *J. Chem. Phys.* **1992**, *96*, 7164.

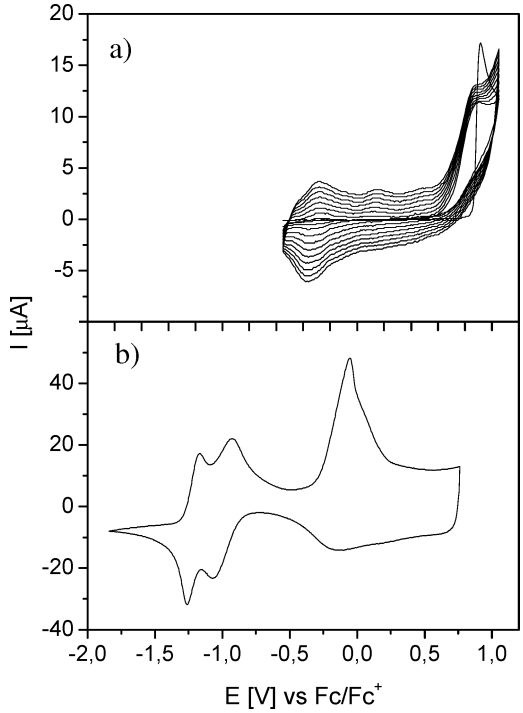

Figure 5. (a) Multisweep voltammogram (10 scans) for the polymerization of PTCDI-EDOT **12** in dichloromethane/TBAHPF (0.1 M) at a scan rate of 100 mV s^{-1}. (b) Electrochemical characterization of corresponding polymer **P12** in acetonitrile/TBAHPF (0.1 M) at a scan rate of 100 mV s^{-1}. All measurements were carried out at room temperature and potentials are given vs Fc/Fc^+.

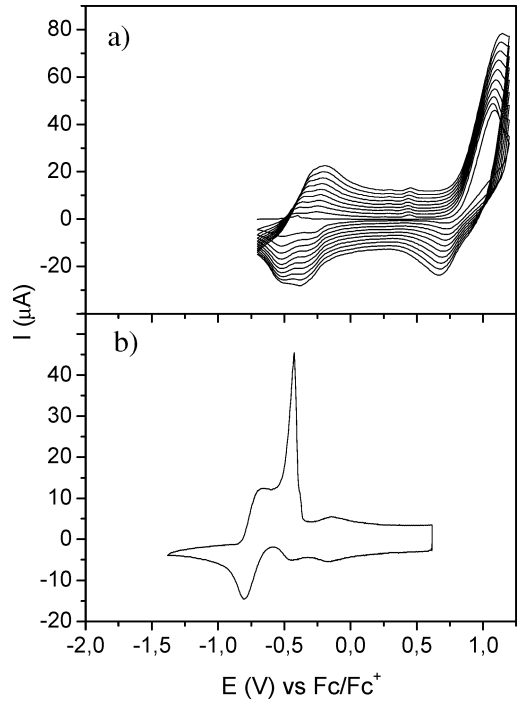

Figure 6. (a) Multisweep voltammogram (10 scans) for the polymerization of TCAQ-EDOT **13** in dichloromethane/TBAHPF (0.1 M) at a scan rate of 100 mV s^{-1}. (b) Electrochemical characterization of corresponding polymer **P13** in acetonitrile/TBAHPF (0.1 M) at a scan rate of 100 mV s^{-1}. All measurements were carried out at room temperature and potentials are given vs Fc/Fc^+.

films of different thicknesses of **P11** were created and electrochemically investigated. In Figure 7 the CVs of P(AQ-EDOT) (**P11**) films formed after 5, 10, and 20 scans are depicted. Typically, the peak currents of the PEDOT redox

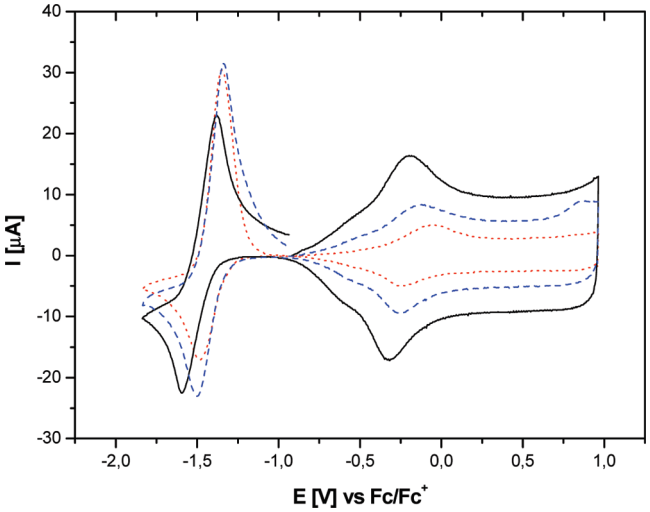

Figure 7. Electrochemical characterization of films of P(AQ-EDOT) (**P11**) electropolymerized with a different number of scans (black solid line, film formed after 20 scans; blue dashed line, after 10 scans; red dotted line, after 5 scans; $CH_3CN/TBAPF_6$ (0.1 M), scan rate of 100 mV s^{-1} on a Pt disk electrode) showing the first reduction and oxidation waves.

wave linearly increase with increasing film thickness. In contrast, in the negative potential regime the peak currents of the acceptor moiety rather decrease, indicating that relatively fewer acceptor units can be electrochemically addressed with increasing film thickness. By integrating the charge flow corresponding to the first redox wave of the AQ unit and to this of the PEDOT backbone, we find a ratio of ≈1.0 for the thinnest film (5 cycles), ≈0.6 for the medium thick film (10 cycles), and ≈0.3 for the thickest film (20 cycles) under investigation. Taking into account that the redox processes of the acceptor unit comprise one electron and these of the backbone 0.3−0.5 per monomer unit, about 30−50% of the AQ units are electrochemically active in the thinnest film, 20−30% in the medium thick film, and only 10−15% in the thickest film. Similar behavior is observed for the acceptor groups in P(PTCDI-EDOT) (**P12**) and P(TCAQ-EDOT) (**P13**).

One rationale for this behavior is a different charging mechanism for the acceptor moieties and the conjugated polymer backbone. Whereas polaronic and bipolaronic delocalization of the charge carriers on the conjugated PEDOT chains is responsible for a rather band-like conduction, for the acceptor units charge transport via activated hopping processes is operative, leading to thickness dependence which is typical for redox polymers.[48]

In the CV of P(PTCDI-EDOT) **P12** the typical two reversible reductions of the perylene unit can be observed at about 200 mV more positive potentials ($E°_{red1} = -1.19$ V, $E°_{red2} = -0.99$ V) than for the related monomer **12** (Figure 5b). This is different than the AQ-functionalized PEDOT **P11** and can be rationalized by more residing positive charges (and higher conductivity) on the PEDOT backbone at the more positive reduction potential of the PTCDI units compared to that of the AQ units.

The CV of TCAQ-functionalized PEDOT **P13** exhibits a completely different shape compared to those of the former

(48) Schäferling, M.; Bäuerle, P. *J. Mater. Chem.* **2004**, *14*, 1132.

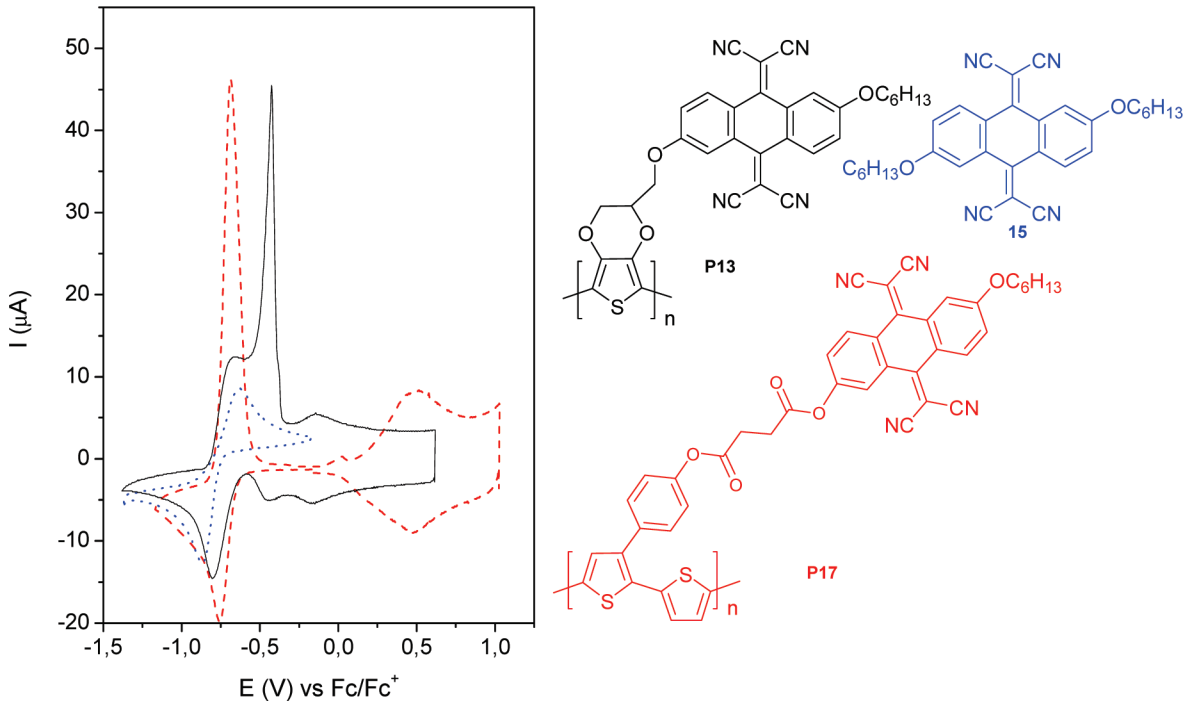

Figure 8. Electrochemical characterization of films of P(TCAQ-EDOT) **P13** (black solid curve) and P(TCAQ-2T) **P17** (red dashed curve) in comparison to reference compound **15** (blue dotted curve); $CH_3CN/TBAPF_6$ (0.1 M), scan rate of 100 mV s^{-1} on a Pt disk electrode.

polymers in which the redox waves of the acceptors are well-separated from those of the conjugated backbone (Figure 6b). At negative potentials, we identify a pair of peaks at $E^p_{red1} = -0.80$ V and $E^p_{ox1} = -0.67$ V, which we assign to the TCAQ group. This is in good agreement with the CV of TCAQ reference compound **15** ($E^p_{red1} = -0.87$ V and $E^p_{ox1} = -0.64$ V) and TCAQ-functionalized polybithiophene **P17** in which the redox wave of the TCAQ group ($E^p_{red1} = -0.75$ V and $E^p_{ox1} = -0.69$ V) is well-separated from that of the polythiophene and therefore allows the assignment (Table 2, Figure 8).[27a] On the other hand, at positive potentials, the typical broad wave of the PEDOT backbone is visible, peaking at $E^p_{ox} = -0.14$ V and $E^p_{red} = -0.16$ V which is comparable to that of polymer **P12**. In the middle of these two redox waves, we find a third very symmetrical pair at $E^p_{red} = -0.44$ V and $E^p_{ox} = -0.42$ V with a considerable sharpening. This peak and its unusual shape is characteristic of a solid-state phenomena where charge is released at an overpotential.[49] This may be due to the close vicinity of TCAQ moieties in the solid state which may allow the formation of weak σ bonds by coupling the radicals residing on the nitrile-bearing carbons.[50] The fact that, in polymer **P17**, used as reference, pendant TCAQ groups are more diluted and decoupled form the polymer backbone prevent the solid-state organization that gives rise to the charge-trapping behavior and therefore this phenomenon is not observed.

From these results it can be concluded that both PEDOT and the acceptor moieties retain their individual electrochemical behavior. No significant interaction can be observed between the donor and acceptor moieties in the ground state. However, from the electrochemical behavior of P(PTCDI-EDOT) it is clear that the redox properties of this material are greatly influenced by the solid-state packing. Furthermore, the unusual behavior observed for the TCAQ derivative can be explained rather in terms of solid-state phenomena than in terms of electronic interactions between the donor and acceptor moieties.

*Optical Properties of the Polymer Films **P11**−**P13** in Comparison to Monomers **11**−**13**.* The absorption spectra of the new acceptor-EDOT systems **11**−**13** in chloroform correspond approximately to a superimposition of the absorption bands belonging to the acceptor moiety and the EDOT system. Thus, this indicates a lack of interaction between both moieties in the ground state, which is in agreement with that observed in the electrochemical characterization of the monomers (Figure 9, Table 3). PTCDI-derivative **12** shows the most red-shifted absorption with a maximum at 527 nm, whereas the TCAQ (396 nm) and AQ moieties (348 nm) absorb at shorter wavelengths. Since the absorption of the Me-EDOT[34] unit is at 259 nm and relatively weak, in the absorption spectra of the hybrid compounds this transition is not resolved and only can be seen as shoulders.

On the other hand, the optical properties of the novel acceptor-PEDOT derivatives **P11**−**P13** in various oxidation states were investigated by spectroelectrochemistry. UV−vis−NIR spectra of the polymer films electrochemically deposited on a platinum working electrode were recorded in situ at various applied potentials in a reflection mode by

(49) (a) Winkler, K.; Costa, D. A.; Hayashi, A.; Balch, A. L. *J. Phys. Chem. B* **1998**, *102*, 9640. (b) Bernhard, S.; Takada, K.; Díaz, D. J.; Abruña, H. D.; Mürner, H. *J. Am. Chem. Soc.* **2001**, *123*, 10265.

(50) For an example of dimerization of TCNQ radical anions via σ bond formation, see: Dong, V.; Endres, H.; Keller, H. J.; Moroni, W.; Nöthe, D. *Acta Crystallogr.* **1977**, *B33*, 2428.

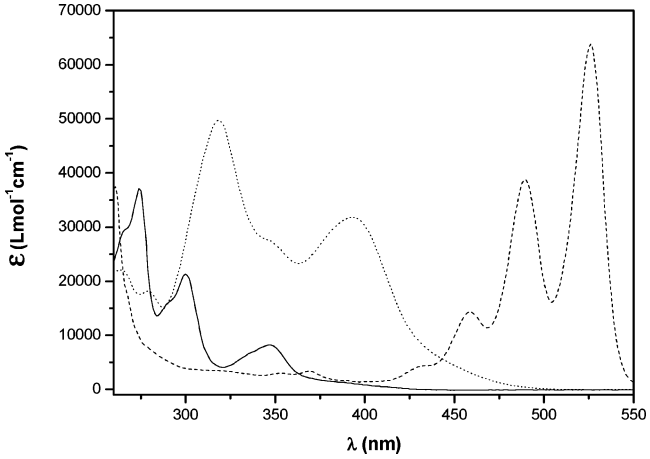

Figure 9. UV−Vis spectra of AQ-EDOT **11** (solid), PTCDI-EDOT **12** (dashed), and TCAQ-EDOT **13** (dotted) in dichloromethane.

means of a fiber optic.[51] In general, the absorption spectrum of PEDOT **P11**−**P13** in a distinct oxidation state approximately corresponds to the superimposition of the spectral features of the PEDOT and the acceptor moiety. In Figure 10 the absorption spectra of all three polymers P(AQ-EDOT) **P11**, P(PTCDI-EDOT) **P12**, and P(TCAQ-EDOT) **P13** in the neutral state are shown. The absorption of **P12** fully covers the visible range and extends up to 850 nm, revealing the superimposition of the absorptions of the individual π-systems. The PEDOT backbone shows typical $\pi-\pi^*$ transition bands at 679 and 623 nm, which are comparable to those of P(Me-EDOT) **P16** (λ = 664, 617 nm). At shorter wavelengths, the characteristic well-structured absorption of the PTCDI system can be identified (λ = 542, 505 nm) which agrees well with the two main absorptions of reference compound **14** (λ = 525, 490 nm) and monomer **12** (λ = 527, 491 nm). In the spectrum of PTCDI-polymer **P12** an additional band at very low energy (λ = 750 nm) appears which we attribute to a charge-transfer band.[52]

Stepwise oxidation of the neutral polymer **P12** (Figure 11) initially leads to a gradual decrease of the intensity of the bands corresponding to the PEDOT moieties in favor of the formation of a rather broad polaron band with a maximum at around 980 nm (Figure 11, dashed line). The intensity of this band gradually decreases at higher potentials with the simultaneous formation of a very broad bipolaron band with an onset at 1000 nm (Figure 11, dotted line) and extending into the near-IR region (λ_{max} > 1600 nm). The absorption bands corresponding to the PTCDI moiety do not significantly alter upon oxidation. This fact clearly indicates that in the range between −0.2 and 1.1 V the polymer is in a state in which the acceptor is neutral and the π-conjugated backbone charged ($PTCDI^0$-$PEDOT^{\bullet+}$).

On the other hand, when the electrode potential was decreased stepwise from −0.2 to −0.7 V, the absorption below 550 nm and above 680 nm decreases in favor of new absorptions peaking at 712, 808, and 994 nm in the regime of 600−1000 nm (Figure 11b, dashed line). Further reduction down to −1.3 V produces a progressive decrease of these new bands and the simultaneous emergence of strong absorptions peaking at 526, 585, and 647 nm (Figure 11b, dotted line). This evolution of the absorption perfectly matches that observed for spectroelectrochemical data obtained for reference PTCDI **14** (Figure 12, Table 3). These bands overlap with that of the PEDOT moiety, thus producing a broad absorption band between 500 and 620 nm. For the reference compound, when the potential is decreased stepwise to −0.7 V, the corresponding peaks are observed at 724, 808, and 992 nm and are due to the formation of PTCDI radical anions, which is in agreement with the electrochemical data. Further reduction down to −1.1 V produces a progressive decrease of these new bands and the simultaneous emergence of strong absorptions peaking at 550, 585, and 609 nm coming from the dianion. In this case, the polymer is in a state in which the PEDOT is neutral and the acceptor charged ($PTCDI^{-\bullet}$-$PEDOT^0$). Rereduction at −0.2 V generates the original absorption spectrum of the polymer film which indicates full reversibility of the process.

In the range between 400 and 1600 nm, the absorption spectra of neutral undoped P(AQ-EDOT) **P11** (Figure 13) and the corresponding P(TCAQ-EDOT) **P13** (Figure 15) mainly show absorption features corresponding to $\pi-\pi^*$ transition in the PEDOT backbone with maxima at 635 and 678 nm for **P11** and at 644 and 691 nm for **P13**.[53] Analogous to that observed with P(PTCDI-EDOT) **P12**, stepwise oxidation leads to a gradual decrease of the intensity of the PEDOT bands in favor of the formation of a rather broad polaron band with a maximum around 1000 nm for **P11** (Figure 13, dashed line) and around 1035 nm for **P13** (Figure 15, dashed line). At higher potentials the intensity of this band gradually decreases with the simultaneous formation of a very broad bipolaron band with an onset at 800−900 nm and extension into the near-IR region (λ_{max} > 1600 nm, Figures 13 and 15, dotted lines).

For PEDOT **P11**, stepwise decrease of the electrode potential from −0.1 to −1.0 V generates new absorption features which are fully developed at −1.0 V with maxima at 420, 527, and around 900 nm (Figure 13, dashed dotted line). These absorptions correlate with the absorption features previously reported for the anthraquinone radical anions (866, 538, and 390 nm).[54] Concerning the TCAQ-endowed polymer **P13**, stepwise decrease of the electrode potential from −0.4 to −1.0 V allows observation of a new absorption feature with a maximum at 540 nm (Figure 15, dashed dotted line). A combined ESR and UV−vis−NIR spectral study performed by Cowan and co-workers[42a] with different TCNQ derivatives showed that absorption with a maximum at 540 nm is produced by both the $TCAQ^{\bullet-}$ radical anion and the

(51) Salbeck, J. *J. Electroanal. Chem.* **1992**, *340*, 169.
(52) Cremer, J.; Mena-Osteritz, E.; Pschierer, N. G.; Müllen, K.; Bäuerle, P. *Org. Biomol. Chem.* **2005**, *3*, 985.
(53) As shown in Figure 9, the absorption spectrum of the anthraquinone moiety only shows absorptions under 400 nm while for the TCAQ system only the onset of the absorption lies above 400 nm. Given that absorption features under 400 nm cannot be registered with the current setup due to absorption from the cell, spectroelectrochemical measurementers can monitor only the presence of new absorption waves upon reduction but not the changes in absorption corresponding to the neutral AQ and TCAQ moieties.
(54) Büschel, M.; Stadler, C.; Lambert, C.; Beck, M.; Daub, J. *J. Electroanal. Chem.* **2000**, *484*, 24.

Table 3. Optical Properties of Acceptor-Functionalized EDOTs 11−13, PEDOTs P11−P13, and Reference Compounds Me-EDOT 16, AQ 6, PTCDI 14, and TCAQ 15 in Various Oxidation States

compound	neutral λ (nm)[a]	PEDOT$^+$ λ (nm)	PEDOT^{2+} λ (nm)	acc.$^{-\bullet}$ λ (nm)	acc.$^{2-}$ λ (nm)
AQ **6**[b]	349, 302, 275			870, 515	
PTCDI **14**[b]	525, 490, 460			992, 808, 724	609, 585, 550
TCAQ **15**[b]	398, 321, 280			522	
Me-EDOT **16**[b]	259				
AQ-EDOT **11**[b]	348, 301, 275, (269)				
PTCDI-EDOT **12**[b]	527, 491, 459, 261				
TCAQ-EDOT **13**[b]	396, 320, 281, 266				
P(AQ-EDOT) **P11**[c]	678, 635, <400 (onset 420)	≈1000	>1600 nm (onset 1000 nm)	900, 527	
P(PTCDI-EDOT) **P12**[c]	679, 623, 542, 505	≈980	>1600 nm (onset 1000 nm)	894, 808, 712	647, 585, 526
P(TCAQ-EDOT) **P13**[c]	691, 644, <400 (onset 463)	≈1035	>1600 nm (onset 1000 nm)	540	
P(Me-EDOT) **P16**[c]	664, 617, 563	≈1015	>1600 nm (onset 1000 nm)		
P(TCAQ-2T) **P17**[c]	490,[d] 350			550	

[a] Maximum underlined, shoulders in brackets. [b] In dichloromethane. [c] 5×10^{-3} mol L^{-1} in CH_3CN/TBAHFP (0.1 M). [d] Corresponding to the polythiophene backbone.

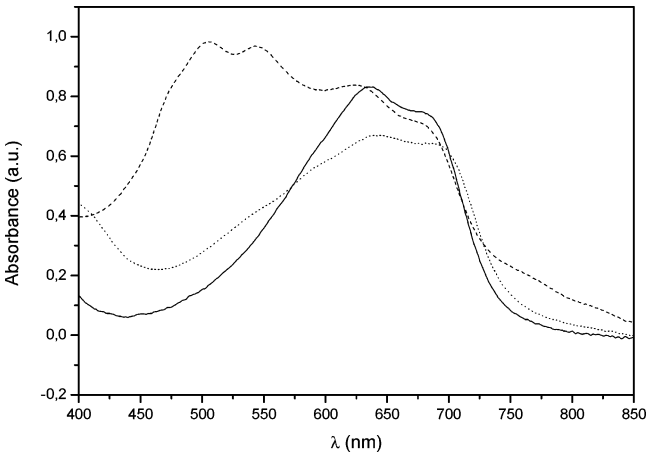

Figure 10. UV−vis spectra of polymer films of P(AQ-EDOT) **P11** (solid), P(PTCDI-EDOT) **P12** (dashed), and P(TCAQ-EDOT) **P13** (dotted) in the neutral state.

TCAQ^{2-} dianion.[55] Compared to the absorption of the radical anion of reference AQ **6**, that of P(AQ-EDOT) **P11** is only slightly red-shifted ($\Delta\lambda$ = 12 nm, Figure 14). The same behavior is observed for the TCAQ-functionalized P(TCAQ-EDOT) **P13** and reference TCAQ **15** ($\Delta\lambda$ = 18 nm, Figure 16).

Conclusion

In summary, we have carried out the straightforward synthesis of a new and versatile chloromethyl-EDOT **3** derivative which provides easy access to functionalized EDOTs and their corresponding PEDOTs endowed with functional groups such as redox active units. With use of this versatile intermediate, EDOT derivatives bearing anthraquinone (**11**), perylenebisimide (**12**), and tetracyanoanthraquinodimethane (**13**) moieties have successfully been synthesized. Characterization of the optical and redox properties of the novel functionalized EDOTs shows that the acceptor moieties and the EDOT core basically are electronically decoupled and retain their individual properties.

(55) It has been reported how radical anions and dianions of some conjugated π-systems absorb in the same wavelength range of the spectrum. For a discussion on this topic, see: Hoijtink, G. J.; Buschow, K. H. J. *J. Chem. Phys.* **1964**, *40*, 2501.

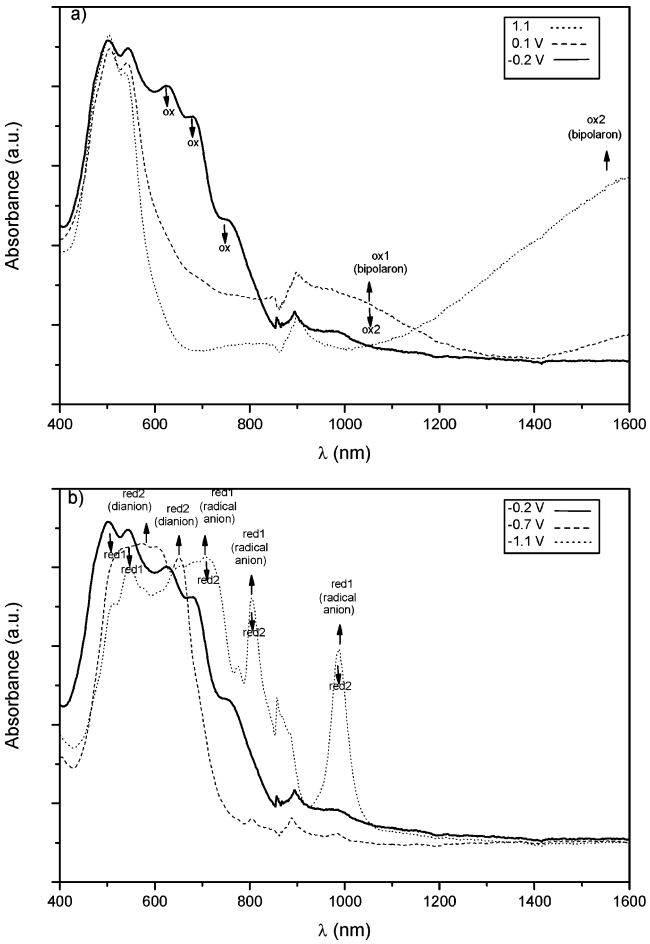

Figure 11. UV−Vis−NIR spectra of **P12** in CH_3CN/TBAHFP (0.1 M): (a) 1.1 V (dotted), −0.2 V (solid), and 0.1 V (dashed) and (b) −0.2 V (solid), −0.7 V (dashed), and −1.1 V (dotted). All potentials vs Ag/AgCl.

Electrochemical polymerization of the novel monomers **11**−**13** has provided polymer films of the corresponding PEDOTs **P11**−**P13** which have been investigated by electrochemical and spectroelectrochemical methods. Cyclic voltammograms of the new polymers show oxidation waves corresponding to the PEDOT system together with the characteristic reduction waves corresponding to the acceptor moieties, indicating that also in the polymer film the pendant

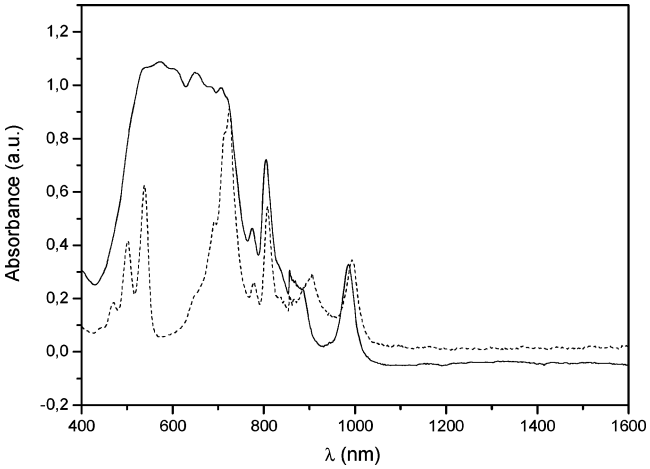

Figure 12. Absorption spectra of P(PTCDI-EDOT) **P12** (solid) and reference PTCDI **14** (dashed) in CH_3CN/ $TBAPF_6$ (0.1 M) at −0.8 V vs Ag/AgCl showing the coincidence of the absorptions corresponding to reduced PTCDI.

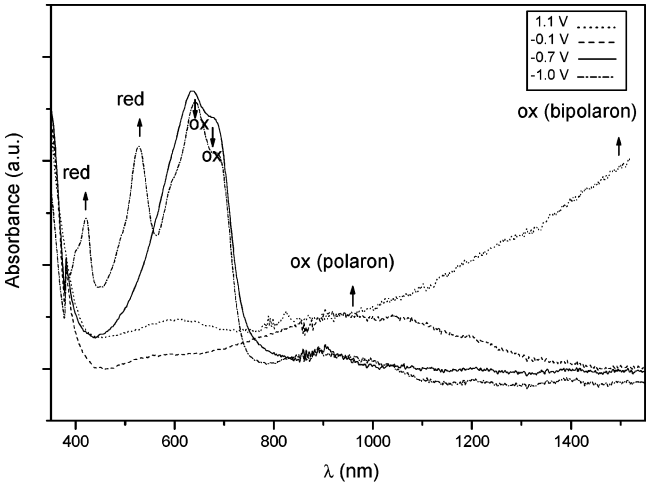

Figure 13. UV−Vis−NIR spectra of P(AQ-EDOT) **P11** in CH_3CN/ TBAHFP (0.1 M) at (a) 1.1 V (dotted), (b) −0.1 V (dashed), (c) −0.7 V (solid), and (d) −1.0 V (dashed dotted). All potentials vs Ag/AgCl.

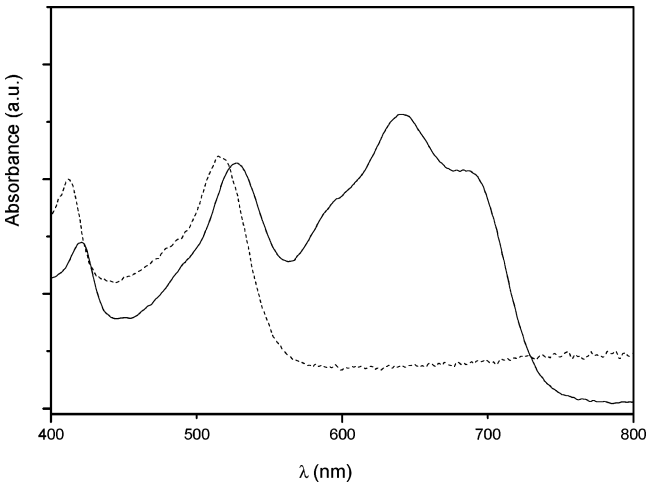

Figure 14. UV−Vis−NIR spectra of P(AQ-EDOT) **P11** (solid) and reference AQ **6** (dashed) at −1.1 V vs Ag/AgCl in CH_3CN/TBAHFP (0.1 M) showing the coincidence of the absorption due to the radical anions of the AQ moieties.

acceptor moieties retain their individual properties, thus having independent redox behavior. Polaronic and bipolaronic delocalization of the charges on the conjugated chains

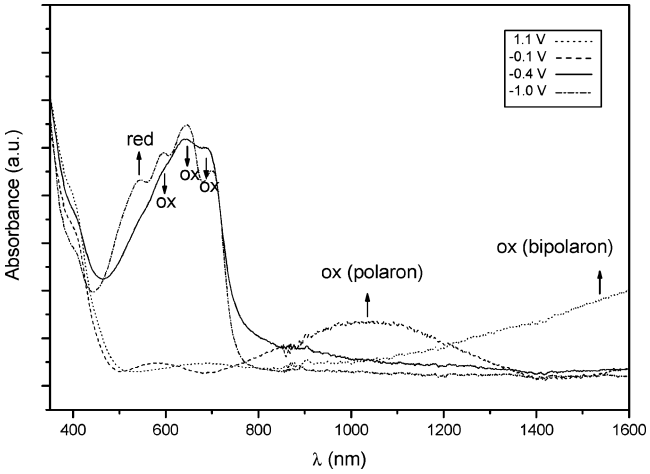

Figure 15. UV−Vis−NIR spectra of P(TCAQ-EDOT) **P13** in CH_3CN/ TBAHFP (0.1 M) at (a) 1.1 V (dotted), (b) −0.1 V(dashed), (c) −0.4 V (solid), and (d) −1.0 V (dashed dotted). All potentials vs Ag/AgCl.

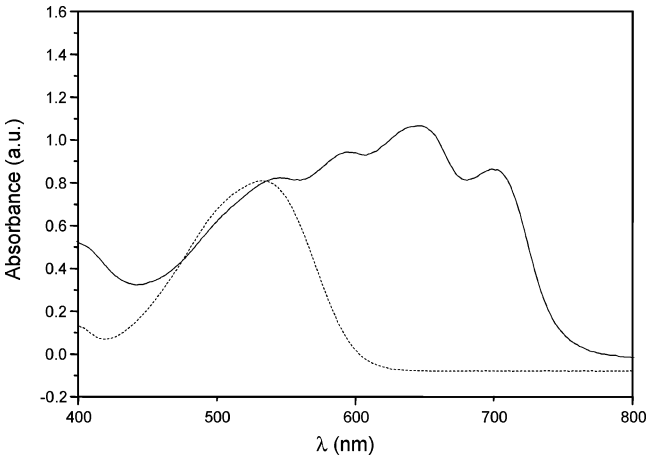

Figure 16. UV−Vis−NIR spectra of P(TCAQ-EDOT) **P13** (solid) and TCAQ reference **15** (dashed) at −1.0 V vs Ag/AgCl in CH_3CN/TBAHFP (0.1 M) showing the absorptions corresponding to the reduced species of the TCAQ moiety.

accounts for a bandlike and p-type conductivity of the PEDOT backbone, while thickness-dependent measurement show that the n-type charge transport involving the acceptor units corresponds rather to an electron-hopping process. Absorption spectra of the hybrid polymers at various oxidation states reveal a superimposition of the spectral features of each individual unit.

The donor−acceptor behavior of these novel functionalized PEDOTs together with the large absorption cross section raise them to potential candidates as intrinsic semiconductors and solar energy harvesters as well as in energy conversion systems.

Experimental Section

Materials. Dimethoxythiophene (**1**)[30] and *N*-(10-nonadecyl)-3,4,9,10-perylenetetracarboxylic 3,4-anhydride-9,10-imide (**8**)[56] were prepared following published procedures. All other chemicals were purchased from Aldrich and used as received without further purification unless otherwise specified. Columm chromatography was performed on Merck Kieselgel 60 silica gel (230−240 mesh). Thin-layer chromatography was carried out on Merck silica gel

(56) Langhals, H.; Sprenger, S.; Brandherm, M. T. *Liebigs Ann.* **1995**, 481.

F-254 flexible TLC plates. Solvents and reagents were dried by the usual methods prior to use and typically used under an inert gas atmosphere.

Characterization. Melting points were measured with an electrothermal melting point apparatus and are uncorrected. FTIR spectra were recorded as KBr pellets in a Shimadzu FTIR 8300 spectrometer. NMR were recorded on a Bruker AC-200, Avance 300, or AMX-400 apparatus as noted, and the chemical shifts were reported relative to tetramethylsilane (TMS) at 0.0 ppm (for ^{1}H NMR) and $CDCl_3$ at 77.16 ppm (for ^{13}C NMR). The splitting patterns are designated as follows: s (singlet), d **(**doublet), and m (multiplet) and the assignments are *Ant* (anthraquinone), *TCAQ* (TCAQ), *Pery* (PTCDI), *Ph* (phenyl), and *Th* (thiophene) for ^{1}H NMR. Mass spectra were recorded with a Varian Saturn 2000 GC-MS and with a MALDI-TOF MS Bruker Reflex 2 (dithranol as the matrix). Elemental analyses were performed on a Perkin-Elmer EA 2400. UV/Vis spectra were taken on a Perkin-Elmer Lambda 19.

Electrochemistry. Cyclic voltammetry experiments were performed with a computer-controlled EG & G PAR 273 potentiostat in a three-electrode single-compartment cell (5 mL). The platinum working electrode consisted of a platinum wire sealed in a soft glass tube with a surface of $A = 0.785$ mm^2, which was polished down to 0.5 μm with Buehler polishing paste prior to use in order to obtain reproducible surfaces. The counter electrode consisted of a platinum wire and the reference electrode was a Ag/AgCl secondary electrode. All potentials were internally referenced to the ferrocene−ferricenium couple. For the measurements, concentrations of 5×10^{-3} mol L^{-1} of the electroactive species were used in freshly distilled and deaerated dichloromethane (Lichrosolv, Merck) and 0.1 M tetrabutylammonium hexafluorophosphate (TBAHFP, Fluka) which was twice recrystallized from ethanol and dried under vacuum prior to use.

Spectroelectrochemistry. Spectroelectrograms were recorded with a Perkin-Elmer Lambda 19 spectrophotometer in conjunction with an EG&G PAR 363 potentiostat. All optical measurements were carried out in a thin layer electrochemical cell according to Salbeck,[51] incorporating a polished platinum disk electrode ($\phi \sim 6$ mm) as the working electrode, a Ag/AgCl wire as the reference electrode, and a platinum sheet as the counter electrode in acetonitrile (HPLC grade, filtered over activated aluminum oxide), TBAHFP (0.1 M). Solutions were deaerated by argon bubbling prior to each experiment, which was run under an argon atmosphere. Spectra were recorded in a reflection mode at the platinum working electrode with the aid of a Y-type optical fiber bundle.

Synthesis of Monomers and Polymers. *2-Chloromethyl-2,3-dihydrothieno[3,4-b][1,4]dioxine (**3**).* To a three-necked flask equipped with an argon purge were added 3,4-dimethoxythiophene **1** (1.14 g, 7.9 mmol), 3-chloro-1,2-propanediol **2** (2.45 g, 22.2 mmol), *p*-toluenesulfonic acid monohydrate (0.151 g, 0.81 mmol), and 27 mL of dry toluene. The solution was heated at 90 °C for 24 h. After this time, another 2.45 g (22.2 mmol) of diol was added, and the solution was heated at 90 °C for another 3 h and was then allowed to cool to room temperature. After removal of the solvent, the remaining crude product was isolated by flash chromatography (silica gel, hexane/dichloromethane 8/2) to give **3** as a white solid in 62% yield. mp 44−45 °C. ^{1}H NMR ($CDCl_3$, 400 MHz): δ 6.37 (AB system, $J_{AB} = 3.71$ Hz, 2H, *Th*), 4.41−4.11 (m, 3H, $-CH_2-OC_{Ar}$), 3.77−3.61 (m, 2H, $-CH_2-Cl$). ^{13}C NMR ($CDCl_3$, 100 MHz): δ 141.16, 140.71, 100.12, 100.11, 72.84 ($-CH-OC_{Ar}$), 65.55 ($-CH_2-OC_{Ar}$), 41.31 ($-CH_2-Cl$). FTIR (KBr, cm^{-1}): ν 2929, 2856, 1489, 1436, 1405, 1252, 1013, 920, 767. MS (EI) (*m*/*z*): 190 (M^+). Anal. Calcd for $C_7H_7ClO_2S$: C, 44.10; H, 3.70; Cl, 18.60; S, 16.82. Found: C, 44.15; H, 3.79; Cl, 18.49; S, 16.83.

*2-Hexyloxy-6-hydroxy-9,10-anthraquinone (**5**).* To a well-stirred solution of 2,6-dihydroxy-9,10-anthraquinone **4** (1.00 g, 4.16 mmol) in 65 mL of anhydrous *N*,*N*-dimethylformamide, 1-bromohexane (0.583 mL, 4.16 mmol), a catalytic amount of potassium iodide and potassium carbonate (575 mg, 4.16 mmol) are added under an argon atmosphere. The mixture is refluxed for 24 h and then allowed to cool, poured with stirring into a 1 N hydrochloric acid solution, and extracted with dichloromethane. The combined organic extracts are dried over anhydrous magnesium sulfate, the solvent evaporated under vacuum, and the residue purified by flash chromatography (silica gel, dichloromethane/methanol 9.5/0.5) to yield 640 mg (48%) of **5** as a yellow solid. mp 88−92 °C. ^{1}H NMR (CD_3OD, 200 MHz): δ 7.87 (d, 2H, $J = 8.3$ Hz, *Ant*), 7.31 (s, 2H, *Ant*), 7.02−6.93 (m, 2H, *Ant*), 4.93 (t, 2H, $-CH_2-OC_{Ar}$), 1.69 (m, 2H, $-CH_2-$), 1.30 (m, 6H, $-CH_2-$), 0.84 (t, 3H, $-CH_3$). ^{13}C NMR (CD_3OD, 50 MHz): δ 183.2 (C═O), 182.9 (C═O), 165.2 ($C_{Ar}-OR$), 164.6 ($C_{Ar}-OR$), 136.9, 136.8, 130.8, 130.3, 127.8, 126.9, 121.6, 121.1, 113.4, 111.6, 69.7 ($-CH_2-OC_{Ar}$), 32.6, 30.0, 26.6, 23.5, 14.3. FTIR (KBr, cm^{-1}): ν 3234, 2932, 2854, 1664, 1570, 1331, 1238, 1150, 1082, 746. MS (EI) (*m*/*z*, %int): 324 (M^+, 48), 240 ($M^+ - C_6H_{13}$, 100), 212 (19). Anal. Calcd for $C_{20}H_{20}O_4$: C, 74.05; H, 6.21. Found: C, 74.15; H, 5.97.

*2-Hexyloxy-6-hydroxy-11,11,12,12-tetracyano-9,10-anthraquinodimethane (**7**).* To a solution of 2-hexyloxy-6-hydroxy-9,10-anthraquinone **5** (600 mg, 1.85 mmol) in 80 mL of dry chloroform, malononitrile (297 mg, 4.5 mmol), titanium(IV) chloride (0.5 mL, 4.6 mmol), and dry pyridine (0.7 mL, 8.7 mmol) are added under an argon atmosphere. The mixture is heated under reflux for 72 h, adding equal amounts of malononitrile, titanium(IV) chloride, and pyridine every 24 h. The crude is then allowed to cool to room temperature and poured with stirring over a mixture of water/ice. The phases are separated and the aqueous layer is extracted with chloroform. The combined organic layers are dried over anhydrous magnesium sulfate and the solvent is evaporated under vacuum. Flash chromatography of the residue (silica gel, hexane/ethyl acetate 6/4) yields 700 mg (89%) of **7** as a yellow solid. mp 193−196 °C. ^{1}H NMR ($CDCl_3$, 200 MHz): δ 8.15 (d, 1H, $J = 8.8$ Hz, *TCAQ*), 8.09 (d, 1H, $J = 8.8$ Hz, *TCAQ*), 7.68 (t, 2H, $J = 2.4$ Hz, *TCAQ*), 7.18−7.08 (m, 2H, *TCAQ*), 4.12 (t, 2H, $-CH_2-OC_{Ar}$), 1.84 (q, 2H, $-CH_2-$), 1.36−1.26 (m, 6H, $-CH_2-$), 0.94 (t, 3H, $-CH_3$). ^{13}C NMR ($CDCl_3$, 50 MHz): δ 162.2, 160.8, 160.5, 160.4, 132.7, 130.0, 129.7, 121.6, 119.3, 118.4, 114.6 (CN), 113.8 (CN), 113.7 (CN), 113.3 (CN), 80.5 ($C(CN)_2$), 80.4 ($C(CN)_2$), 69.4 ($-CH_2-OC_{Ar}$), 31.5, 29.0, 25.6, 22.7, 14.0. FTIR (KBr, cm^{-1}): ν 3312, 3020, 2930, 2858, 2226, 1605, 1541, 1466, 1329, 1310, 1246, 1215, 1170, 756. MS (EI) (*m*/*z*, %int.): 420 (M^+, 20), 336 ($M^+ - C_6H_{13}$, 100), 311 (35), 308 (23), 55 (22). Anal. Calcd for $C_{26}H_{20}N_4O_2$: C, 74.27; H, 4.79; N, 13.32. Found: C, 74.36; H, 5.10; N, 13.03.

*N-(4-Hydoxyphenyl)-N′-(10-nonadecyl)perylene-3,4,9,10-bis(carboximide) (**10**).* A mixture of *N*-(10-nonadecyl)-3,4,9,10-perylenetetracarboxylic 3,4-anhydride-9,10-imide[56] **8** (326 mg, 0.5 mmol), 4-aminophenol **9** (218 mg, 2 mmol), $Zn(OAc)_2$ (73 mg, 0.4 mmol), and 2 g of imidazol is heated at 180 °C for 2 h under an argon atmosphere. After cooling to room temperature, the mixture is treated with 100 mL of an aqueous 10% hydrochloric acid solution. The solid is collected by filtration, washed with another portion of acid solution, and thoroughly washed with water and finally with methanol. The remaining solid is dried under vacuum and further purified by flash chromatography (silica gel, dichloromethane/methanol 9.5/0.5) to yield **10** (268 mg, 72%) as a waxy deep red solid. mp > 350 °C. ^{1}H NMR ($CDCl_3$, 300 MHz): δ 8.64 (d, 4H, $J = 7.92$ Hz, *Pery*), 8.54 (d, 4H, $J = 7.92$ Hz, *Pery*), 7.13 (d, 2H, $J = 8.71$ Hz, *Ph*), 6.96 (d, 2H, $J = 8.71$ Hz, *Ph*), 5.13 (m, 1H, $-CH-N$), 2.20 (m, 2H, $-CH_2-$), 1.84 (m, 2H, $-CH_2-$), 1.19 (m,

28H, $-CH_2-$), 0.78 (t, 6H, $-CH_3$). ^{13}C NMR ($CDCl_3$, 75 MHz): δ 164.40, 157.61, 135.38, 134.64, 132.19, 131.5, 130.02, 129.79, 129.78, 126.87, 126.73, 126.66, 123.71, 123.55, 123.51, 116.69, 55.25, 32.68, 32.20, 29.88, 29.61, 27.34, 22.99, 14.41. FTIR (KBr, cm^{-1}): ν 2924, 2852, 1697, 1655, 1595, 1576, 1508, 1344, 1255, 1146, 748. MS (ESI) (*m*/*z*): 748 (M^+). Anal. Calcd for $C_{49}H_{51}N_2O_5$: C, 78.67; H, 6.87; N, 3.74. Found: C, 78.22; H, 6.72; N, 3.73.

*2-[((6-Hexyloxy-9,10-anthraquinone)-2-yl)oxymethyl]-2,3-dihydrothieno[3, 4-b][1,4]dioxine (AQ-EDOT, **11**).* Under an argon atmosphere, a mixture of chloromethyl-EDOT **3** (389 mg, 2.0 mmol), 2-hexyloxy-6-hydroxy-9,10-anthraquinone **5** (664 mg, 2.0 mmol), potassium carbonate (582 mg, 4.0 mmol), and a catalytic amount of potassium iodide is heated at 100 °C in 40 mL of anhydrous *N*,*N*-dimethylformamide. After 24 h, an equal amount of chloromethyl-EDOT **3** is added and the reaction is allowed to stand for another 48 h. The crude is allowed to reach room temperature and treated with a 1 M aqueous solution of hydrochloric acid. The mixture is extracted with dichloromethane and the organic extracts dried over anhydrous magnesium sulfate and then evaporated under vacuum. The residue is purified by flash chromatography (silica gel, hexane/dichloromethane 1/9) to yield 736 mg (77%) of **11** as a yellow solid. mp 153−154 °C. ^1H NMR ($CDCl_3$, 300 MHz): δ 8.16 (d, 1H, $J = 8.6$ Hz, *Ant*), 8.13 (d, 1H, $J = 8.6$ Hz, *Ant*), 7.64 (d, 1H, $J = 2.6$ Hz, *Ant*), 7.61 (d, 1H, $J = 2.6$ Hz, *Ant*), 7.24−7.14 (m, 2H, *Ant*), 6.30 (AB system, $J_{AB} = 3.72$ Hz, 2H, *Th*), 4.51 (m, 1H, $-CH-OC_{Ar}$), 4.36−4.02 (m, 6H, $-CH_2-OC_{Ar}$), 1.76 (q, 2H, $-CH_2-$), 1.49−1.25 (m, 6H, $-CH_2-$), 0.82 (t, 3H, $-CH_3$). ^{13}C NMR ($CDCl_3$, 75 MHz): δ 181.90 (C=O), 164.15, 162.82, 141.23, 140.86, 135.90, 129.77, 129.73, 127.81, 126.87, 121.03, 110.54, 100.19, 71.60 ($-CH-OC_{Ar}$), 68.86 ($-CH_2-OC_{Ar}$), 66.69 ($-CH_2-OC_{Ar}$), 65.55 ($-CH_2-OC_{Ar}$), 31.50, 28.98, 25.61, 22.57, 14.00. FTIR (KBr, cm^{-1}): ν 2931, 2868, 1684, 1584, 1506, 1458, 1336, 742. MS (MALDI-TOF) (*m*/ *z*): 479 ($M^+ + 1$). Anal. Calcd. for $C_{27}H_{26}O_6S$: C, 67.76; H, 5.48. Found: C, 67.61; H, 5.59.

*2-[(N′-(10-nonadecyl)perylene-3,4,9,10-biscarboximide-N-yl)4-phenoxymethyl]-2,3-dihydrothieno[3,4-b][1,4]dioxine (PTCDI-EDOT, **12**).* Under an argon atmosphere, a mixture of chloromethyl-EDOT **3** (105 mg, 0.54 mmol), *N*-(4-hydoxyphenyl)-*N*′-(10-nonadecyl)perylene-3,4,9,10-bis(carboximide) **10** (200 mg, 0.27 mmol), potassium carbonate (75 mg, 0.54 mmol), and a catalytic amount of potassium iodide in 45 mL of anhydrous N,N-dimethylformamide is heated at 100 °C for 72 h. The crude is allowed to reach room temperature and treated with a 1 M aqueous solution of hydrochloric acid. The red precipitate is collected, washed thoroughly with another portion of acid solution, with water, and with methanol, and dried under vacuum. Flash chromatography of the crude (silica gel, dichloromethane/methanol 99/1) yields 82 mg (34%; 54% based on recovered reactive) of **12** as a deep red solid. mp 233−234 °C (dec). ^1H NMR ($CDCl_3$, 400 MHz): δ 8.75 (d, $J = 8.04$ Hz, 4H, *Pery*), 8.67−8.63 (m, 4H, *Pery*), 7.29 (d, $J = 8.78$ Hz, 2H, *Ph*), 7.11 (d, $J = 8.78$ Hz, 2H, *Ph*), 6.38 (AB system, $J_{AB} = 3.89$ Hz, 2H, *Th*), 5.23 (m, 1H, −CH−N), 4.6−4.2 (m, 5H, $-CH_2-OC_{Ar}$), 2.27 (m, 2H, $-CH_2-$), 1.89 (m, 2H, $-CH_2-$), 1.56−1.20 (m, 28H, $-CH_2-$), 0.83 (t, 6H, $-CH_3$). ^{13}C NMR ($CDCl_3$, 100 MHz): δ 163.73, 158.31, 141.43, 141.11, 135.13, 131.84, 129.55, 128.35, 126.68, 126.42, 123.30, 123.04, 115.41, 100.04, 100.00, 99.82, 71.79 ($-CH-OC_{Ar}$), 66.40 ($-CH_2-OC_{Ar}$), 65.87 ($-CH_2-OC_{Ar}$), 54.85 (−CH−N), 32.37, 31.85, 29.69, 29.25, 26.98, 22.72, 14.07. FT-IR (KBr): ν 2922, 2852, 1699, 1653, 1595, 1344, 1254 cm^{-1}. MS (MALDI-TOF) (*m*/*z*): 903 $[M + H]^+$. Anal. Calcd for $C_{56}H_{58}N_2O_7S$: C, 74.47; H, 6.47; N, 3.10. Found: C, 74.68; H, 6.59; N, 2.98.

*2-[((6-Hexyloxy-11,11,12,12-tetracyanoanthraquinodimethane)-2-yl)-oxymethyl]-2,3-dihydrothieno[3,4-b][1,4]dioxine (TCAQ-EDOT, **13**).* To a solution of the 9,10-anthraquinone-functionalized EDOT **11** (300 mg, 0.63 mmol) in 60 mL of dry chloroform, malononitrile (125 mg, 1.89 mmol), titanium(IV) chloride (0.21 mL, 1.9 mmol), and pyridine (0.31 mL, 3.8 mmol) are added under an argon atmosphere. The mixture is heated under reflux for 72 h, adding equal amounts of malononitrile, titanium(IV) chloride, and pyridine every 24 h. The crude is then allowed to cool to room temperature and poured with stirring over a mixture of water/ice. The phases are separated and the aqueous layer is extracted with chloroform. The combined organic phase is dried over anhydrous magnesium sulfate and the solvent evaporated under vacuum. Flash chromatography of the residue (silica gel, dichloromethane) yields 214 mg (62%) of **13** as a yellow solid. mp 149−151 °C. ^1H NMR ($CDCl_3$, 300 MHz): δ 8.12 (d, 1H, $J = 8.8$ Hz, *TCAQ*), 8.10 (d, 1H, $J = 8.8$ Hz, *TCAQ*), 7.75 (d, 1H, $J = 2.4$ Hz, *TCAQ*), 7.70 (d, 1H, $J = 2.4$ Hz, *TCAQ*), 7.24−7.14 (m, 2H, *TCAQ*), 6.31 (AB system, $J_{AB} = 3.92$ Hz, 2H, *Th*), 4.50 (m, 1H, $-CH-OC_{Ar}$), 4.30−4.01 (m, 6H, $-CH_2-OC_{Ar}$), 1.77 (q, 2H, $-CH_2-$), 1.49−1.18 (m, 6H, $-CH_2-$), 0.84 (t, 3H, $-CH_3$). ^{13}C NMR ($CDCl_3$, 75 MHz): δ 171.15, 162.35, 161.04, 159.94, 159.82, 141.14, 140.68, 132.81, 132.57, 129.72, 129.68, 122.91, 121.64, 118.59, 118.40, 113.63 (CN), 113.50 (CN), 113.42 (CN), 113.29 (CN), 100.55, 81.42 ($C(CN)_2$), 80.95 ($C(CN)_2$), 69.29 ($-CH-OC_{Ar}$), 67.06 ($-CH_2-OC_{Ar}$), 65.35 ($-CH_2-OC_{Ar}$), 60.39 ($-CH_2-OC_{Ar}$), 31.42, 28.83, 25.54, 22.54, 14.19. FTIR (KBr, cm^{-1}): ν 2924, 2852, 2222, 1576, 1558, 1489, 1338, 1244. MS (MALDI-TOF) (*m*/*z*): 575 ($M^+ + 1$). Anal. Calcd for $C_{33}H_{26}N_4O_4S$: C, 68.97; H, 4.56; N, 9.75. Found: C, 68.85; H, 4.67; N, 9.78.

*General Procedure for the Electrosynthesis of Functionalized PEDOTs (**P11**−**P13**).* A dichloromethane solution of tetrabutylammonium hexafluorophosphate (0.1 M) was deoxygenated with dry argon for 15 min. Monomers were electropolymerized by successive scanning at a concentration of 5×10^{-3} M in the above-mentioned dichloromethane/tetrabutylammonium hexafluorophosphate solution. The modified working electrodes were dried in air and electrochemically characterized in an electrolyte free of monomer.

*Electrosynthesis of P(AQ-EDOT) **P11**.* Electropolymerization of monomer AQ-EDOT **11** was carried out following the general procedure, by successive scanning between −1.0 and 1.1 V. Anal. Calcd for $(C_{27}H_{24}O_6S)_n$: C, 68.05; H, 5.08. Found: C, 67.92; H, 5.21.

*Electrosynthesis of P(PTCDI-EDOT) **P12**.* Electropolymerization of monomer PTCDI-EDOT **12** was carried out following the general procedure, by successive scanning between −0.6 and 1.1 V. Anal. Calcd for $(C_{56}H_{56}N_2O_7S)_n$: C, 74.64; H, 6.26; N, 3.11. Found: C, 74.42; H, 6.36; N, 3.02.

*Electrosynthesis of P(TCAQ-EDOT) **P13**.* Electropolymerization of monomer TCAQ-EDOT **13** was carried out following the general procedure, by successive scanning between −0.6 and 1.1 V. Anal. Calcd for $(C_{33}H_{24}N_4O_4S)_n$: C, 69.22; H, 4.22; N, 9.78. Found: C, 69.37; H, 4.31; N, 9.67.

Acknowledgment. We thank the DAAD, Comunidad de Madrid (Ref. GR/MAT/0628/2004 and PR45/ 05-14167), MCyT (Ref. CTQ2004-03760), and Ministerio de Educación y Ciencia of Spain and DAAD (Acciones Integradas, Ref. HA2005-0116) for financial support. R.G. is indebted to the "Programa Ramón y Cajal" and R.B to the Comunidad de Madrid for a doctoral fellowship.

CM0602085